GCA TECHNICAL REPORT NO. 65-25-N

LANGMUIR PROBES FOR MEASUREMENTS IN THE IONOSPHERE

L. G. SMITH

Bedford, Massachusetts

CONTRACT NO. NASw-1141

PREPARED FOR

NATIONAL AERONAUTICS AND SPACE ADMINISTRATION

HEADQUARTERS

WASHINGTON, D. C.

OCTOBER 1965

GCA Technical Report No. 65-25-N*

LANGMUIR PROBES FOR MEASUREMENTS IN THE IONOSPHERE

L. G. Smith

Contract No. NASw-1141

October 1965

*A contribution to the "Technique Manual on Electron Density and Temperature Measurements in the Ionosphere," edited by Dr. K. Maeda and published by COSPAR.

GCA CORPORATION
GCA TECHNOLOGY DIVISION
Bedford, Massachusetts

Prepared for

NATIONAL AERONAUTICS AND SPACE ADMINISTRATION
Headquarters
Washington 25, D. C.

ABSTRACT

12867

The design and use of a DC probe for rocket measurements of electron density and electron temperature in the ionosphere is described. The probe is based on the Langmuir probe technique in a form which is particularly suitable for the investigation of features of the ionosphere involving steep gradients, such as sporadic E. The potential value of the probe in the D region is indicated.

author

TABLE OF CONTENTS

LIST OF ILLUSTRATIONS

LANGMUIR PROBES FOR MEASUREMENTS IN THE IONOSPHERE

By L. G. Smith
GCA Corporation

INTRODUCTION

The Langmuir probe technique for the measurement of electron density and electron temperature was one of the first experiments to be carried on sounding rockets. Since the first use on rockets in 1946 and 1947 [1]* and, since 1958, on satellites [2], the method has become one of the most important tools of the ionosphere scientist complementing the radio sounding techniques.

The theory and application of the Langmuir probe for measurements in the ionosphere is described in this manual for the information of other scientists who may wish to compare their measuring techniques with this one. It is not possible to discuss in detail the many variations of the probes based on the Langmuir technique but an attempt has been made to indicate the major variations and the relation between them.

Section 1 contains a simplified presentation of probe theory and its fundamental limitations, which, fortunately, are not serious for ionospheric measurements. The particular application to rocket and satellite measurements is discussed in Section 2. The potential value of the probe in the D region (50 to 90 km) is noted although the Langmuir theory is not strictly valid at such low altitudes due to the relatively high neutral gas density.

The design and construction of an instrument for use in sounding rockets is given in Section 3. This instrument alternates the normal Langmuir technique with a second mode which has been found more suitable for studies of sporadic E and other highly localized features of the electron density profile.

The most significant deviation from Langmuir probe theory (which has been encountered) concerns the actual value of the electron random current density. The observations indicate values that are lower than the theoretical values by a factor approaching an order of magnitude. Some uncertainty is introduced by the difficulty of identifying exactly the point at plasma potential but this is not enough to account for the low electron current. It is believed that the explanation of the discrepancy can be attributed to the effect of the earth's magnetic field. This point is by no means cleared up and pending further evidence, either experimental or theoretical, the probe is being used empirically. Since the measurement of electron temperature is remarkably independent of such factors as electrode geometry and the geomagnetic field, the technique is used with confidence.

---

*The numbers in [ ] throughout the text represent reference numbers.

1. LANGMUIR PROBE THEORY

Retarding Potential Analysis

The use of a probe in studying plasmas was originally put on a sound theoretical basis by Langmuir and his colleagues more than thirty years ago [3]. Experimentally, an electrode is inserted into the plasma and the current to it is determined as a function of the potential of the electrode. From the resulting current-voltage characteristic the electron energy distribution and the electron density are obtained.

When the electrode is exactly at the potential of the plasma the electron current to it is determined by the random thermal motions of the electrons in the gas. From kinetic theory the number of electrons striking unit area per second is $n_e\overline{v_e}/4$ where n_e is the electron density and $\overline{v_e}$ the electron mean velocity. Since each electron carries a charge e, the electron random current density j_e is given by

$$j_e = n_e e\, \overline{v_e}/4 \tag{1}$$

The mean electron velocity $\overline{v_e}$ is related to the electron temperature T_e by

$$\overline{v_e} = (8kT_e/\pi m_e)^{\frac{1}{2}} \tag{2}$$

where k is the Boltzmann constant and m_e is the electron mass. The use here of electron temperature implies a Maxwellian distribution, i.e., thermal equilibrium. Numerically,

$$\overline{v_e} = 6.21 \times 10^5\ T_e^{\frac{1}{2}}\ \text{cm/sec} \tag{3a}$$

or

$$\overline{v_e} = 6.69 \times 10^7\ V_e^{\frac{1}{2}}\ \text{cm/sec} \tag{3b}$$

where V_e is the electron energy in volts.

The variation of electron random current density as a function of electron density is shown in Figure 1 for three values of electron energy.

As the electrode is made negative with respect to the plasma, only those electrons with energies greater than the retarding potential can strike the electrode. For retarding potentials the electron current density j is given by

$$j = j_e \exp(eV/kT_e) \tag{4}$$

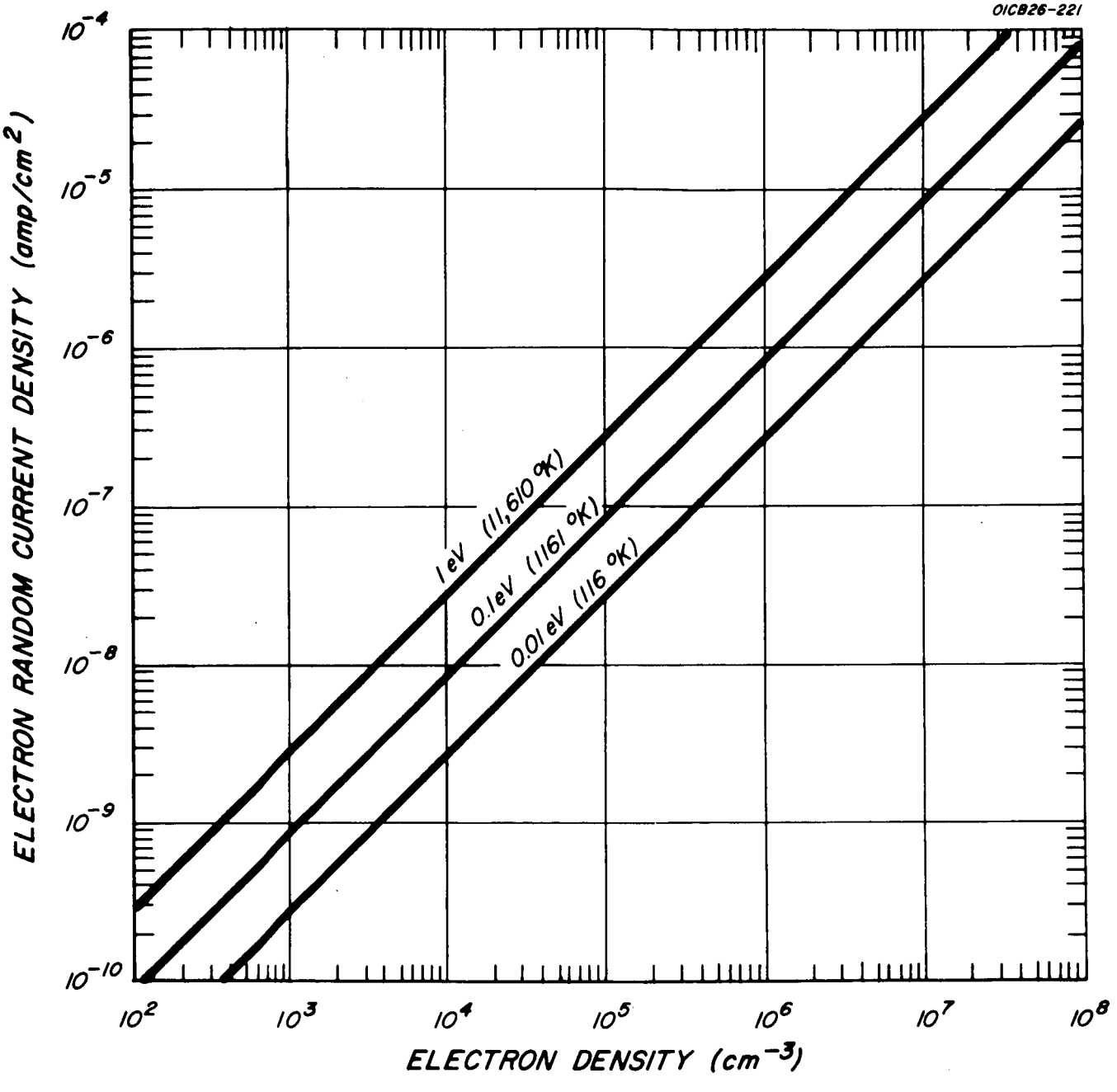

Figure 1. Electron random current density as function of electron density for three values of electron energy.

where V is the retarding potential.

Equations (1), (2), and (4) define the theory of the Langmuir probe technique in its simplest possible terms.

Plasma Sheath

Important to the basic theory of the Langmuir probe, though not appearing explicitly in the formulae quoted above, is the concept of the plasma sheath — the space charge region adjacent to the electrode. It will be realized that the sheath has zero thickness (i.e., does not exist) when the electrode is at plasma potential. The concept of the sheath is important in two respects: (1) it provides a criterion for the validity of the technique; namely, that the mean free path be large compared with the sheath thickness, and (2) it provides a method of computing the current-voltage curves for accelerating potentials. Such calculations have been given in detail by Mott-Smith and Langmuir [4].

The thickness of the plasma sheath varies with the potential of the electrode, but the scale of thickness can conveniently be expressed in terms of the plasma properties by the Debye shielding length h, defined by the equation

$$h = \left(\frac{kT_e}{4\pi n_e e^2}\right)^{\frac{1}{2}} = 6.90\ (T_e/n_e)^{\frac{1}{2}} \text{ cgs units} \tag{5}$$

The variation of Debye shielding length with electron density is shown in Figure 2 for three values of electron energy.

The current-voltage characteristic for accelerating potentials is a function of the shape and size of the electrode. Exact expressions are available when the dimensions of the electrode are very large or very small compared with the Debye shielding length:

(1) Large plane

$$j = j_e \tag{6}$$

(2) Long thin cylinder

$$j = j_e\left\{\frac{2}{\pi^{\frac{1}{2}}}\left(\frac{eV}{kT_e}\right)^{\frac{1}{2}} + \exp\left(\frac{eV}{kT_e}\right)\operatorname{erf}\left(\frac{eV}{kT_e}\right)^{\frac{1}{2}}\right\} \tag{7}$$

(3) Small sphere

$$j = j_e\left(1 + \frac{eV}{kT_e}\right) \tag{8}$$

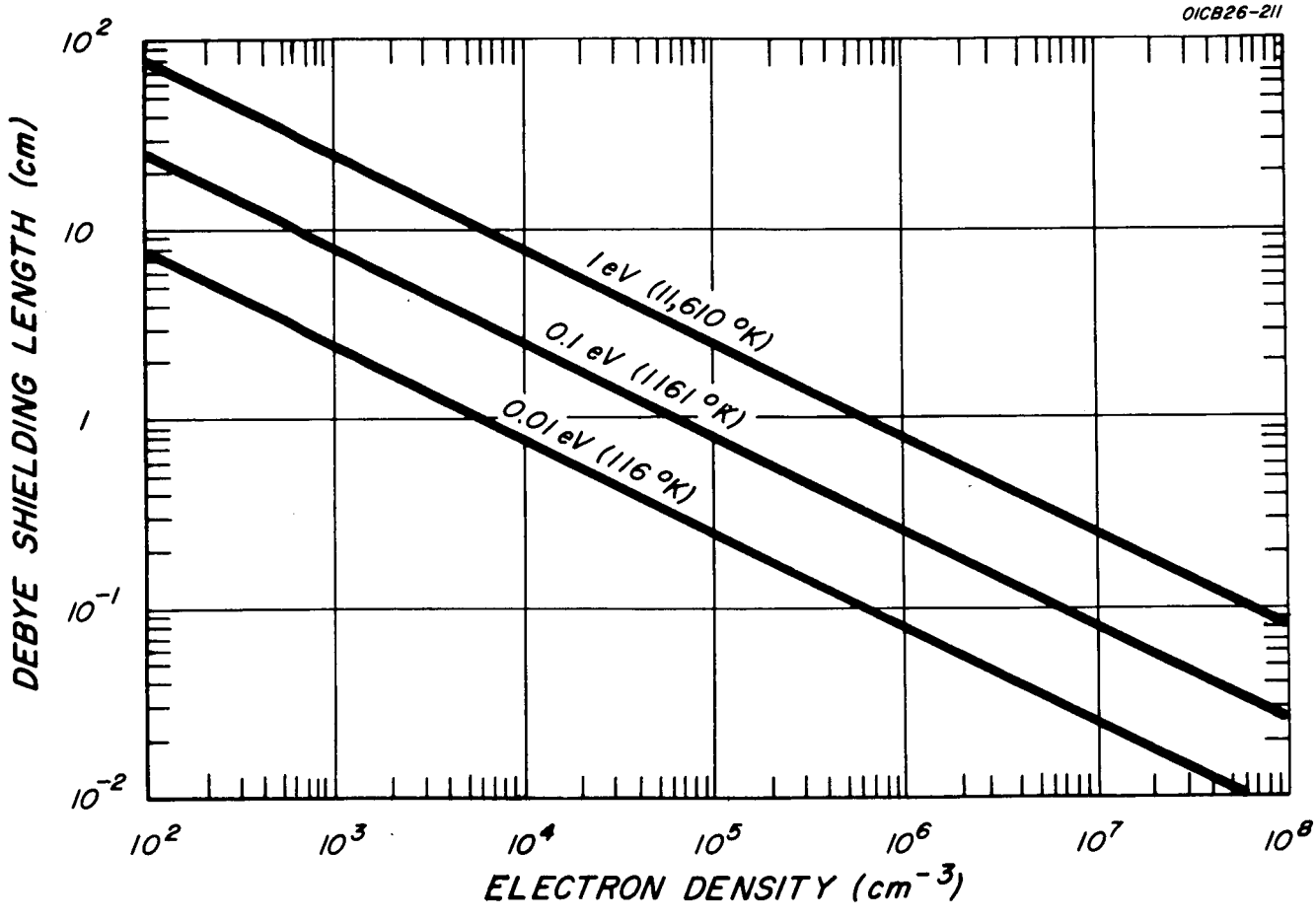

Figure 2. Debye shielding length as a function of electron density for three values of electron energy,

A normalized semi-log plot of electron current versus voltage is shown in Figure 3 for these three electrode configurations. The large plane and small sphere are limiting cases; all other electrode shapes result in plots falling within the region between these two curves. As noted before, for retarding potentials the current density is independent of electrode shape and the semi-log plot results in a straight line where slope gives the electron temperature. The point at which the electrode is at plasma potential is readily identified by the change in slope on this semi-log plot.

Non-Maxwellian Energy Distribution

When the electron energy distribution is not Maxwellian the log j-V plot is not linear in the retarding potential region. The current-voltage curve may still be analyzed, however, to give the actual electron energy distribution. A convenient method, due to Druyvesteyn [5], uses the second derivative d^2j/dV^2. Expressed in terms of the electron energy in volts, V_e, the distribution function $F(V_e)$ is given by

$$F(V_e) = \frac{1}{n}\frac{dn}{dV_e} = \frac{(8m)^{\frac{1}{2}}}{e^{3/2}} V^{\frac{1}{2}} \frac{d^2j}{dV^2} \tag{9}$$

Several methods are available for obtaining the second derivative electrically though only recently has the theory of such methods been discussed generally [6].

A simple method has been used by Takayama, et al. [7], in which a small ac signal is superimposed on the sweep voltage producing a change in the current averaged with respect to the ac signal. If i_o is the current into the probe at a given retarding potential V_o then the addition of an ac signal V cos ωt, where $|V| < |V_o|$, increases the current from i_o to a new value

$$i = i_o J_o (ieV/kT) \tag{10}$$

where $J_o(ieV/kT)$ is the zeroth order Bessel function for a pure imaginary argument. Some values of the function are given in Table 1.

TABLE 1

VALUES OF $J_o(ieV/kT)$

eV/kT	0	1	2	3	4
$J_o(ieV/kT)$	1.000	1.266	2.280	4.881	11.302

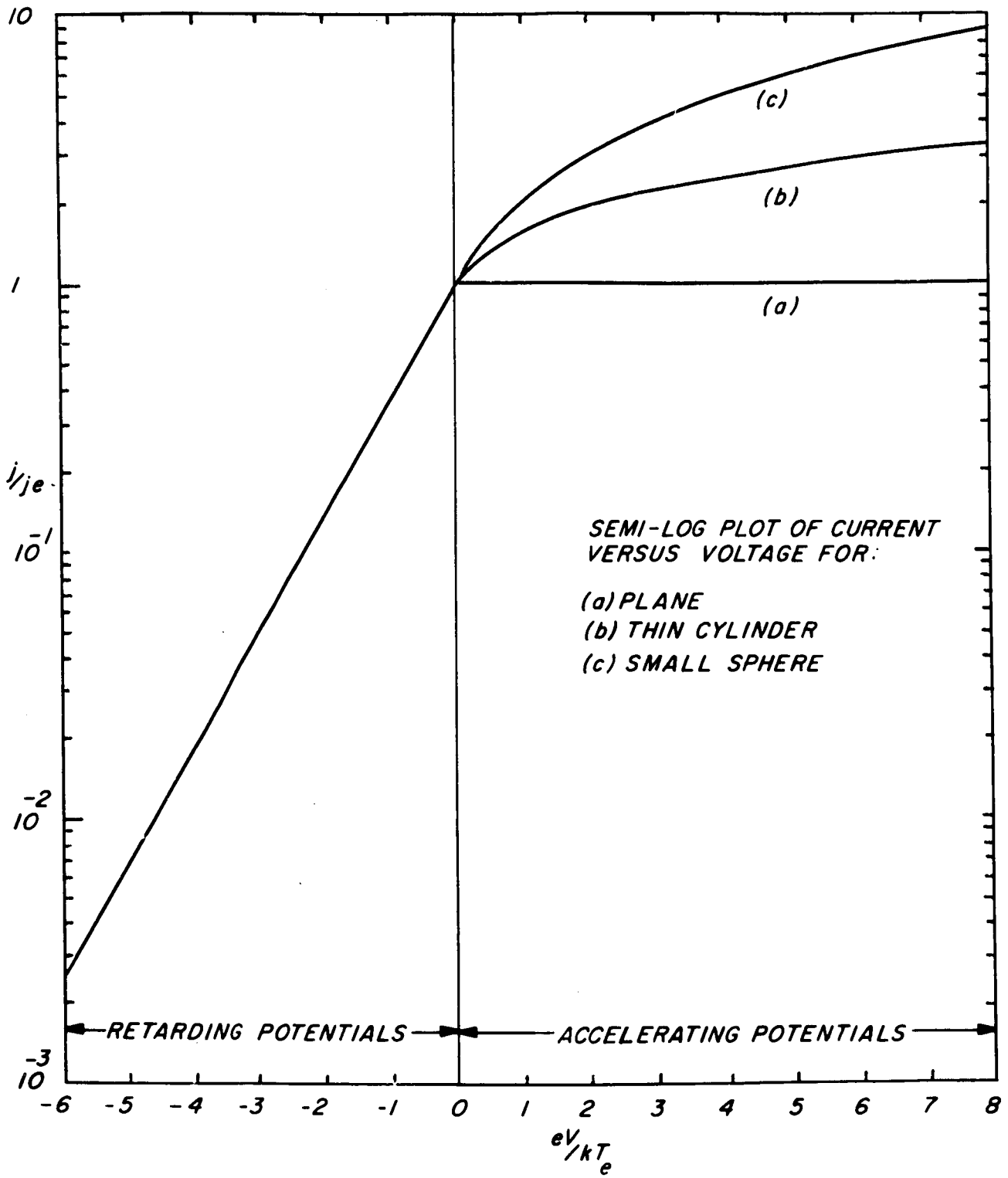

Figure 3. Theoretical semi-log plot of electron current.

A measurement of the ratio of the current with and without the ac signal present gives the value of J_o and, since V is known, leads immediately to the electron temperature T. The frequency of the ac signal may be in the audio frequency or radio frequency range but in any case should be no greater than 10 percent of the plasma frequency in order to avoid resonance effects.

A more elaborate probe of this type has been used by Boyd and Willmore [8] on the satellite Ariel. Two small ac signals having amplitudes of 50 to 100 mv and frequencies of 500 c/s and 3 kc/s are added to the normal sweep voltage of the probe. The curvature of the current-voltage characteristic produces components of current to the probe having frequencies equal to the sum and difference of the two applied ac signals. The components at the higher frequency (3.0 kc/s) are selected by a tuned amplifier and the depth of modulation measured. This gives the ratio of the first and second derivatives of the curve which, for the case of a Maxwellian distribution, is equal to the electron energy (in volts, if practical units are used).

Positive Ion Current

The current to the electrode is the sum of currents due to positive ions as well as electrons. (Here and later we postulate the absence of negative ions.) The positive ion component of the current is given by Equations (1), (2), and (4) when the sign of the potential is reversed and j_+, T_+, $\overline{v_+}$, and m_+ are substituted for the corresponding quantities j_e, T_e, $\overline{v_e}$, and m_e. Because of the much greater mass of the positive ion (for atomic oxygen $m_+/m_e = 16 \times 1836$), the positive ion random current density is smaller than the electron random current density by a factor of about 170. This has the important consequence that correcting the observed current to obtain the electron current involves a small quantity.

Floating Potential

The potential at which the total electrode current is zero is of considerable significance in rocket and satellite measurements. This is a negative potential V_f known as the floating (or wall) potential, because any isolated conductor or insulator will come to this potential under electron and positive ion bombardment. Since the positive ion and electron currents must be equal in magnitude, the value of V_f is given by

$$j_+ = j_e \exp[-(eV_f/kT_e)] \tag{11}$$

or

$$eV_f = kT_e \log_e (j_e/j_+) = 5.1\ kT_e \tag{12}$$

for $(j_e/j_+) = 170$. Thus the floating potential is almost equal to five times the electron energy when both are expressed in volts. This value is very insensitive to the particular values assumed for ion mass and ion temperature.

Bi-Polar Probe

An important development of the Langmuir probe technique is the floating double-probe method [9]. Two probes are inserted in the plasma and the current flowing between them is measured as a function of the voltage difference without reference to the actual potential of the plasma. The method was originally developed to minimize the reaction of the probes on the plasma under investigation. It is also used on rockets and satellites where no reference potential is available.

The two probes comprising the bi-polar arrangement are not necessarily equal in size or shape. If the inequality in size of the two probes is considerable then the smaller can be treated as a single probe, the other providing a constant reference potential. An analysis of the current-voltage characteristic as a function of the area ratio (σ) is given in the appendix.

Three modes of operation of a bi-polar probe are determined by the magnitude of the area ratio of the probes σ and the ratio of electron to ion random current density j_e/j_+:

(1) $1 \leq \sigma < j_e/j_+$. In this mode of operation neither probe can be driven positive with respect to the plasma. Hence the electron random current density is not measured. In addition the value of electron temperature obtained is representative of these electrons with energies greater than a certain value. There is very little to recommend this mode of operation.

(2) $j_e/j_+ \leq \sigma < 10\ j_e/j_+$. Electron and ion random current densities are measured. The electron temperature is obtained for a complete spectrum of electron energies and it is possible to test for a Maxwellian distribution.

(3) $10 j_e/j_+ \leq \sigma$. The merits of the previous mode are present with the advantage that the data evaluation is somewhat simplified. Its disadvantage is that, for a given total probe area, the probe current is rather small.

The optimum area ratio for the bi-polar probe is considered to be $\sigma = 10 j_e/j_+$.

Another result of this analysis is that the value of electron temperature obtained is not affected by the area ratio of the electrodes.

Limitations of Probe Theory

There are restrictions on the use of the Langmuir probe. The following criteria must be met when applying the probe to the study of discharges in gases:

(1) The probe dimensions must be small in comparison to significant changes in potential over the space it occupies.

(2) The current drawn by the probe must not disturb the plasma.

(3) There must be no collisions within the sheath (i.e., the mean-free path must be large compared with the sheath thickness).

(4) There must be no production of electrons by impact, photo-emission, etc., at the probe surface.

(5) There must be no negative ions in the plasma.

(6) Contact potential differences must be constant.

(7) Radio-frequency fields must be absent (because of the possibility of exciting plasma oscillations).

(8) The geometry of the probe arrangement must be clearly defined.

Within the limitations imposed by these criteria, the Langmuir probe has proved an elegant and powerful tool for the study of low pressure discharges. Attempts have been made to extend the use of the probe to other conditions, particularly to higher pressures, (i.e., short mean free paths) but the interpretation under these conditions is uncertain.

2. THE PROBE IN THE IONOSPHERE

Useful Altitude Range

The ionosphere in the E region provides an almost ideal plasma for application of the Langmuir probe technique. Values of some of the relevant quantities are given in Table 2. Below about 90 km the theory of the probe is invalid because two important factors do not meet the criteria previously given: (1) the mean free path is not large compared with the Debye length and (2) negative ions are present in significant numbers.

The use of the probe in the F region is limited by photoemission. The photoelectric current density from a tungsten surface exposed to unattenuated solar radiation is about 4×10^{-9} amp/cm^2. This is equal to the random current for a value of electron density of about 4×10^3 cm^{-3} (at a temperature of 10^{3o}K). This gives an upper limit to the height range for daytime measurements of about 1000 km.

Environment of the Vehicle

The atmosphere in the vicinity of a rocket or satellite is disturbed from its quasi-equilibrium state. The electron density, probably more than any other property, is susceptible to considerable modification. If a probe is to succeed in measuring ambient electron density it is of the utmost importance that the interaction of the vehicle and the ionosphere be understood. Considered to be of potential importance are:

(1) Ionization by rf excitation, increasing the electron density.

(2) Absorption of rf energy, increasing the electron temperature.

(3) Rectification at the antennas, modifying the vehicle potential.

(4) Escaping gas and outgassing, tending to dilute the plasma.

(5) Vehicle motion, modifying the spatial density distribution.

(6) Shock wave ionization, increasing the electron density.

(7) Photoemission from the vehicle, modifying the vehicle potential.

(8) Magnetic fields (including the geomagnetic field) modifying the probe current.

Effects associated with the rf transmitters, when, as usually is the case, the data is telemetered, with gas contaminating the environment and with vehicle motion, can in practice be made negligible by suitable design of the experiment. Photoemission (in daytime) and the geomagnetic field are left as being inherent

TABLE 2

SELECTED QUANTITIES RELEVANT TO THE LANGMUIR PROBE
IN THE IONOSPHERE

Height, h km	150	250	350	700
Electron Concentration, n_e cm^{-3} (noon)	2×10^5	1×10^6	2×10^6	2×10^5
*Temperature, T^oK	1031	1415	1445	1812
Molecular Weight, M (ions)	28	16	16	16
Ratio, $\overline{v_e}/\overline{v_+}$ (= j_e/j_+)	228	170	170	170
Electron Mean Velocity, $\overline{v_e}$ cm sec^{-1}	2.0×10^7	2.3×10^7	2.4×10^7	2.7×10^7
Ion Mean Velocity, $\overline{v_+}$ cm sec^{-1}	8.8×10^4	1.4×10^5	1.4×10^5	1.6×10^5
Electron Random Current Density, j_e amp cm^{-2}	1.6×10^{-7}	9.2×10^{-7}	1.9×10^{-6}	2.1×10^{-7}
Ion Random Current Density, j_+ amp cm^{-2}	7.0×10^{-10}	5.4×10^{-9}	1.1×10^{-8}	1.2×10^{-9}
Floating Potential, V_f volt	-0.48	-0.63	-0.64	-0.80
Debye Shielding Length, h cm	0.50	0.26	0.19	0.66

*Values up to 700 km from 1959 ARDC Model Atmosphere.

limitations on a probe measurement of electron density. The theory of operation of the probe should be modified to incorporate these effects.

Vehicle Motion

It is in the nature of rocket and satellite-borne instruments that they are moving with significant velocity relative to the plasma. It is important to consider the effect of this relative motion on the operation and interpretation of the probe. Two separate aspects of the motion can be distinguished.

Effect of motion on ion current.— The velocity of a sounding rocket (say 1 km/sec) is comparable with, and the velocity of a satellite (say 8 km/sec) is appreciably greater than, the mean velocity of the ions (of the order of 1 km/sec), although both are very small compared with the mean velocity of electrons (about 200 km/sec). The ion current to an electrode is increased due to relative motion whereas the electron current is not appreciably changed. An exact expression has been given by Sagalyn, et al. [10], for a spherical electrode. This is shown graphically in Figure 4. When the vehicle velocity, v, equals the mean ion velocity, $\overline{v_+}$, the current is increased about 40 percent above the value with no relative motion. For a satellite having a velocity of 8 times the mean ion velocity the current is increased by a factor of about 8. Since the ion current is still small compared with the electron current the motion of the vehicle does not affect the retarding potential analysis for electrons.

Rarefaction in the vehicle wake.— A further factor affecting the design of a probe experiment results from the local disturbance of ion and electron density due to rarefaction in the wake of a body traveling through the plasma with a velocity comparable with or greater than the mean ion velocity [11]. Although the electrons have sufficient velocity individually to penetrate this region, the absence of a neutralizing positive space charge prevents the build-up of an appreciable electron concentration, with the result that the electron density distribution also shows a rarefaction in the wake of the vehicle. This effect showed up clearly in an early flight (Nike-Cajun 10.25) which included in the payload an electrode in the form of a disc flush-mounted in the cylindrical section of the payload housing. This rocket slowly executed a large precession cone while spinning more rapidly on its longitudinal axis. It was found that the current to this probe was modulated in synchronism with the spin, being a minimum with the electrode at the trailing side of the payload. The probe on a rocket or satellite should therefore be located so that the probability of its passage through the rarefied vehicle wake is minimized.

Magnetic Field

A factor which is not considered in simple probe theory is the effect of a magnetic field. In the E region the radius of gyration (Larmor radius) for electrons in the geomagnetic field is about 1 cm. Since this dimension is less than the mean free path of the electrons and comparable with the size of the

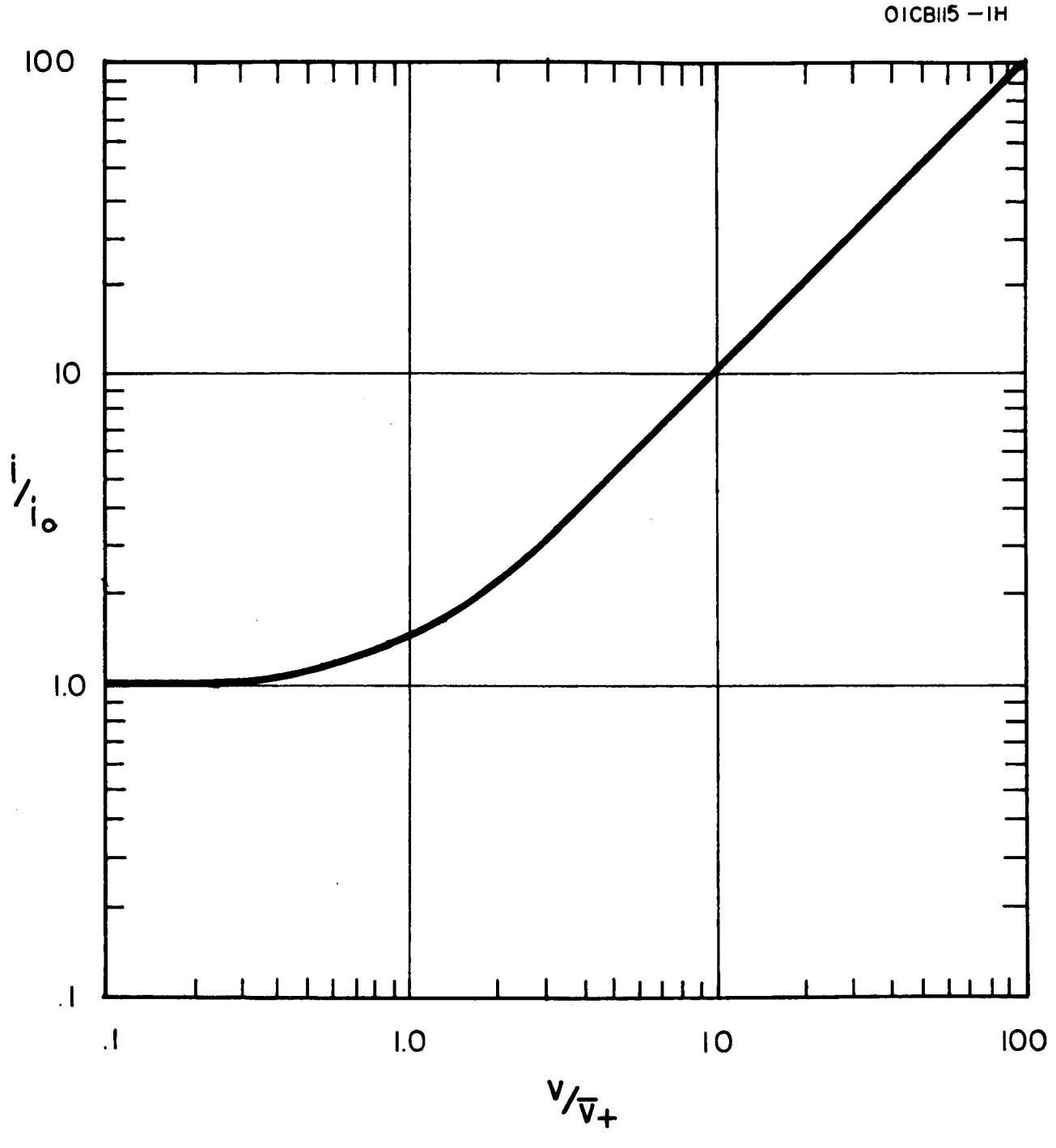

Figure 4. Effect of vehicle velocity on ion current.

probe normally used, the motions of electrons into or away from the probe must be profoundly affected. In some unpublished lecture notes F. F. Chen states that in a magnetic field weak enough so that the ion Larmor radius is large compared with the probe radius and the Debye length and hence that j_+ is not affected, but strong enough so that the electron Larmor radius is comparable to or smaller than the relevant dimensions, the ratio j_e/j_+ falls to 10 or 20. In the absence of a magnetic field the ratio j_e/j_+ has a value of about 200. Thus the geomagnetic field would tend to decrease the observed value of j_e by an order of magnitude. There is some evidence that this is the case. Chen also states that, in the presence of a weak magnetic field the retarding potential analysis would not be affected and the resulting value of electron temperature should be correct. It should be pointed out, however, that there exists no comprehensive mathematical treatment of the Langmuir probe theory in the presence of even a weak magnetic field. This is of no particular concern in respect of the use of the probe to measure electron density where other methods (such as radio-frequency techniques) can be used to check and calibrate the equipment. There is no direct method of measuring electron temperature, however, which is not based on Equation (4).

Measurement of Ionospheric Irregularities

An important aspect of probes carried by rockets and satellites is their ability to resolve the fine structure of the medium. This is most important initially in respect to electron density where less direct methods, e.g., radio star scintillations, have indicated that significant variations exist having typical dimensions as small as 200 meters.

A basic weakness of the conventional Langmuir probe technique is its poor time resolution. This follows because a complete sweep of potential of the electrode leads to only a single value of electron density and of electron temperature. In practice, the sweep duration is limited by two factors: (1) a bandwidth of the measuring device and (2) the bandwidth of the telemetry system. A sweep duration of the order of one second is generally convenient for rocket and satellite measurements although this can be reduced to about 0.1 sec at the expense of elaborating the instrument. However, an alternative method has been developed and used with considerable success.

The method is experimentally very simple but somewhat more difficult to justify on theoretical grounds. It consists in changing the program of the voltage applied to the probing electrode from one of consecutive sweeps to a program in which occasional sweeps are separated by periods of fixed voltage. In recent flights using the technique, the program consisted of a sweep voltage of -2.7 to +2.7 volt (duration 0.5 sec) alternating with a fixed voltage of +2.7 volt (duration 1.5 sec), Figure 5.

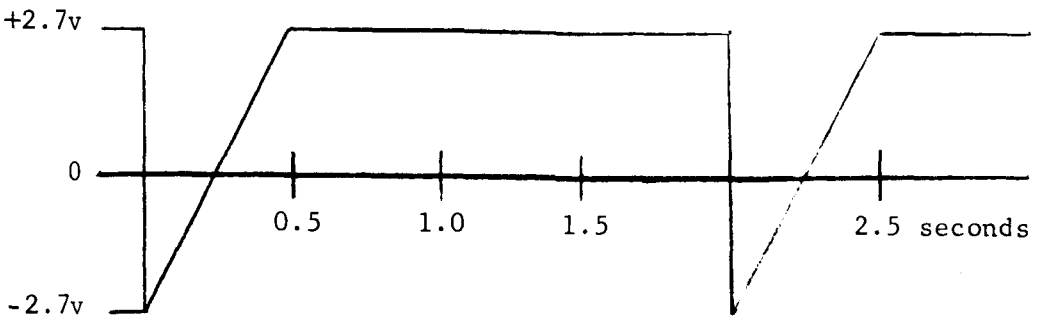

Figure 5. Probe voltage program.

The probe current at fixed potential is proportional to electron density. The only assumption made is that electron temperature is constant; the current is proportional to the average velocity of the electrons and hence varies as $(T_e)^{\frac{1}{2}}$. The proportionality of current to electron density has been verified in the flight of a rocket (Nike-Apache 14.31) which carried a probe and a cw propagation experiment, the latter prepared by S. J. Bauer (Goddard Space Flight Center).

The distance resolution of the instrument used in this way depends on the vehicle velocity and the bandwidth of the system (including telemetry). For a rocket with a velocity of 1 km/sec and a bandwidth of 1 kc/sec the distance resolution is 1 meter, more than adequate for present applications. In a satellite having a velocity of 8 km/sec the bandwidth required to give a distance resolution of 80 meters would be 100c/sec.

Telemetry Requirements

The bandwidth required in the telemetry channel is principally determined by the lower limit of electron temperatures. In the lower E region values of electron temperature as low as 300°K have been measured and it is probably desirable that the limit for the measurement be set at 100°K. This corresponds to a mean electron energy of about 0.01 volt. Now the sweep voltage applied to the probe has a slope of 10 volts/sec which is equal to an increment of 0.01 volt in 1 msec. This indicates that the bandwidth should be about 1 kc/sec if the exponentially rising current in the retarding potential region is to be transmitted.

The output of the instrument is an analog voltage and may be transmitted by any standard telemetry system. It has been found that the FM/FM system is the most convenient manner of telemetering for this instrument when used on sounding rockets.

Contact Potential

A feature of the current-voltage plots obtained on rocket flights using the bi-polar arrangement is that they do not pass through the origin of coordinates. Thus with zero potential applied to the electrode (either nose or side) the current is not zero. Similarly the electrode must be made positive with respect to the rocket body to reduce the probe current to zero. Comparison of actual and theoretical plots shows that the curve is displaced along the voltage axis rather than the current axis. Thus the effect is due to a bias voltage appearing in the probe circuit. This bias voltage usually lies between 0.5 and 1.0 volt and may change slowly with time, Figure 6.

The bias is believed to be an effect produced by contact potential though no complete explanation can be given. It has been observed in laboratory tests that, while there is no bias voltage when an ohmic (carbon) resistor is used as a load, the bias appears when a very dilute solution of common salt is used. This was also noticed on one occasion (Nike-Cajun 10.108); the bias voltage appeared as salt spray accumulated on the rocket during the pre-launch period. (Incidentally, the leakage current due to the salt spray disappeared at launch.)

The contact potential presumably arises from the use of dissimilar metals for the two electrodes of the bi-polar arrangement. The change during flight is believed to be due to the heating of the electrodes during the launch phase.

The actual value of the contact potential is of no consequence in the normal retarding potential analysis since the potentials are automatically referred to plasma potential. It does, however, somewhat affect the fixed-voltage mode of operation of the probe since any change in contact potential produces an equal change in the potential of the probe with respect to the plasma. When this effect is important a correction may be obtained from the individual current-voltage plots.

Electrode Configuration

It was noted earlier that the variation of current for retarding potentials is independent of the shape of the electrode. Therefore, electron density and electron temperature can be determined, in principle, using an electrode of any shape. The most common forms used in gas discharges are spheres or long thin cylinders. Ichimiya, et al. [12], have used rings and spherical mesh probes to reduce the photoemission current.

In rocket and satellite applications two electrodes are used. Spencer, et al. [13], have found a "dumbbell" arrangement of identical spherical electrodes satisfactory for measurement of electron temperature and positive ion density. The symmetrical arrangement does not allow the direct measurement of electron density, however. The asymmetrical arrangement in which the rocket or satellite body is the larger electrode is more frequently used. In this case the smaller electrode may be treated as a single probe and the shape again is not critical. Bourdeau, et al. [14], has used a disc mounted on the

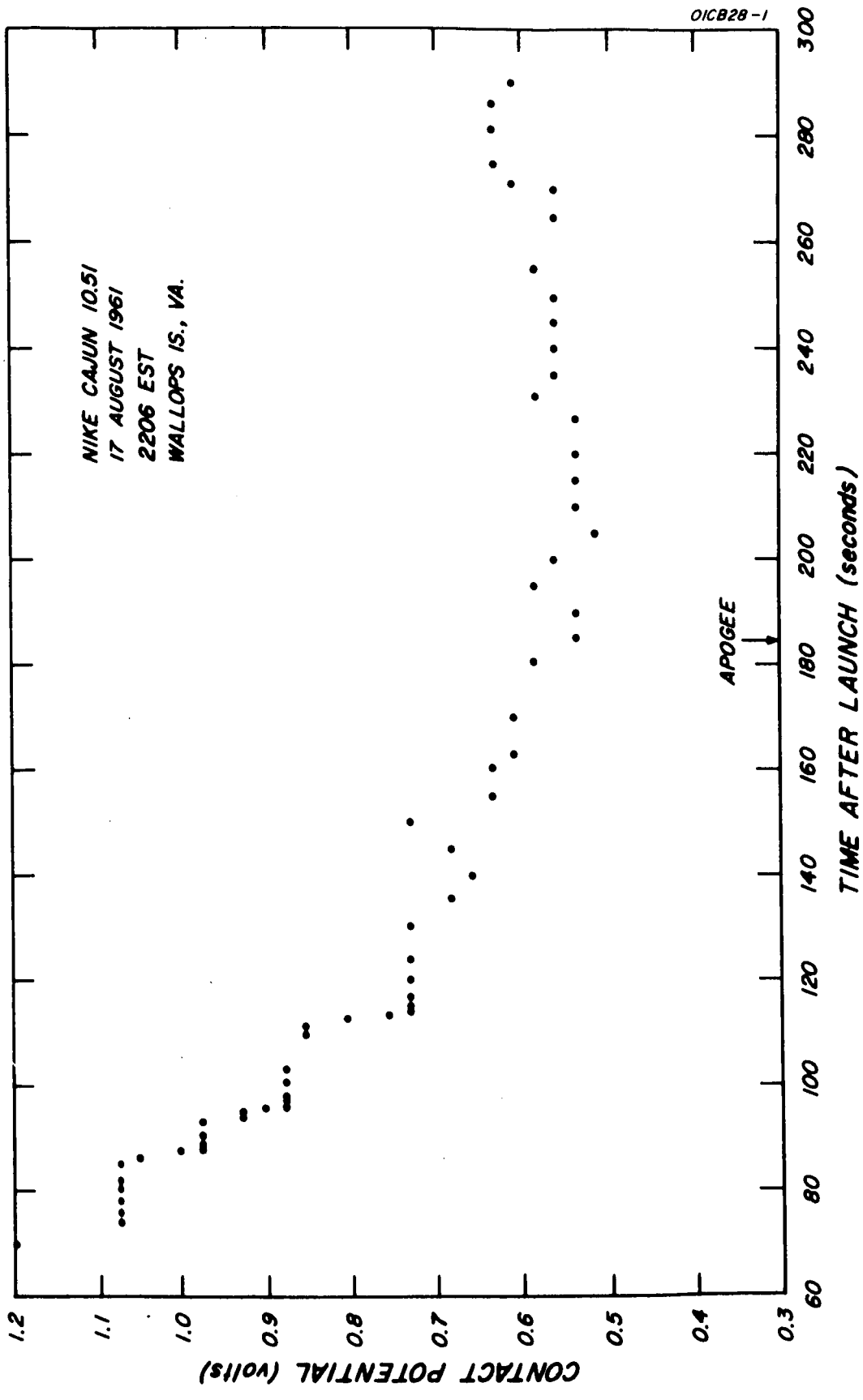

Figure 6. Variation of contact potential.

body of a satellite for measurement of electron temperature. Willmore, et al. [15], have used a plane disc 2 cm in diameter at the end of a boom 1 meter long extending from a satellite. On the same satellite a similar disc mounted on the body gave measurements of electron temperature in good agreement with those from the boom-mounted electrode.

Probes with Grids

The addition of a grid between the probe (collector) and the ambient plasma allows the electron and positive ion currents to be measured separately. This technique was first successfully used by Boyd [16] in laboratory experiments and later adapted to rocket and satellite instruments. In Boyd's arrangement a single grid is used; with the collector biased positive (+48V) the electron current is measured and with the collector biased negative (-60V) the positive ion current is measured. Thus the electron and positive ion current can be measured as functions of the grid potential. This technique is superior to the simple probe for determination of the electron energy distribution since the problem of subtracting the positive ion current is avoided and consequently the electron current determined to larger retarding potentials.

The first satellite use of such a probe (known as an ion-trap) is due to Gringauz and co-workers [2,17]. The collector and grid are both spherical and are mounted at the end of a boom 65 cm long. The grid is 10 cm in diameter and has a transparency factor of 63 percent. The collector 3 cm in diameter, concentric with the grid, is maintained at a negative potential of -150V with respect to the satellite body. This potential ensures that all positive ions entering the ion-trap are attracted to the collector. The collector current, i, is determined by the potential of the grid, V, with respect to the plasma, the effective cross sectional area A' of the grid (i.e., the actual cross section reduced by the transparency factor) and the mean ion energy V_o, due to the satellite velocity, and has the form

$$i = n_+ e A' (1 + V/V_o) \qquad (13)$$

Thus the current varies linearly with potential and is reduced to zero when the grid is at a positive potential equal to $-V_o$ (5.33 volts for atomic oxygen and a vehicle velocity of 8×10^5 cm/sec). The cut-off potential gives a measurement of the ion-mass, and the instrument can be regarded as a low-resolution mass spectrometer; it is adequate to resolve O^+, He^+ and H^+, for example, which makes it useful at satellite altitudes. The finite ion temperature reduces the sharpness of the cut-off, as shown in Figure 7, and provides a method of determining positive ion temperature. In addition the current to the grid is measured and analyzed in the manner of a simple Langmuir probe to give electron density and electron temperature.

The use of a spherical ion-trap on rockets has been described by Sagalyn, et al. [10]. The rocket and positive ion velocities are now comparable and the computation of collector current is more difficult. In their instrument, the

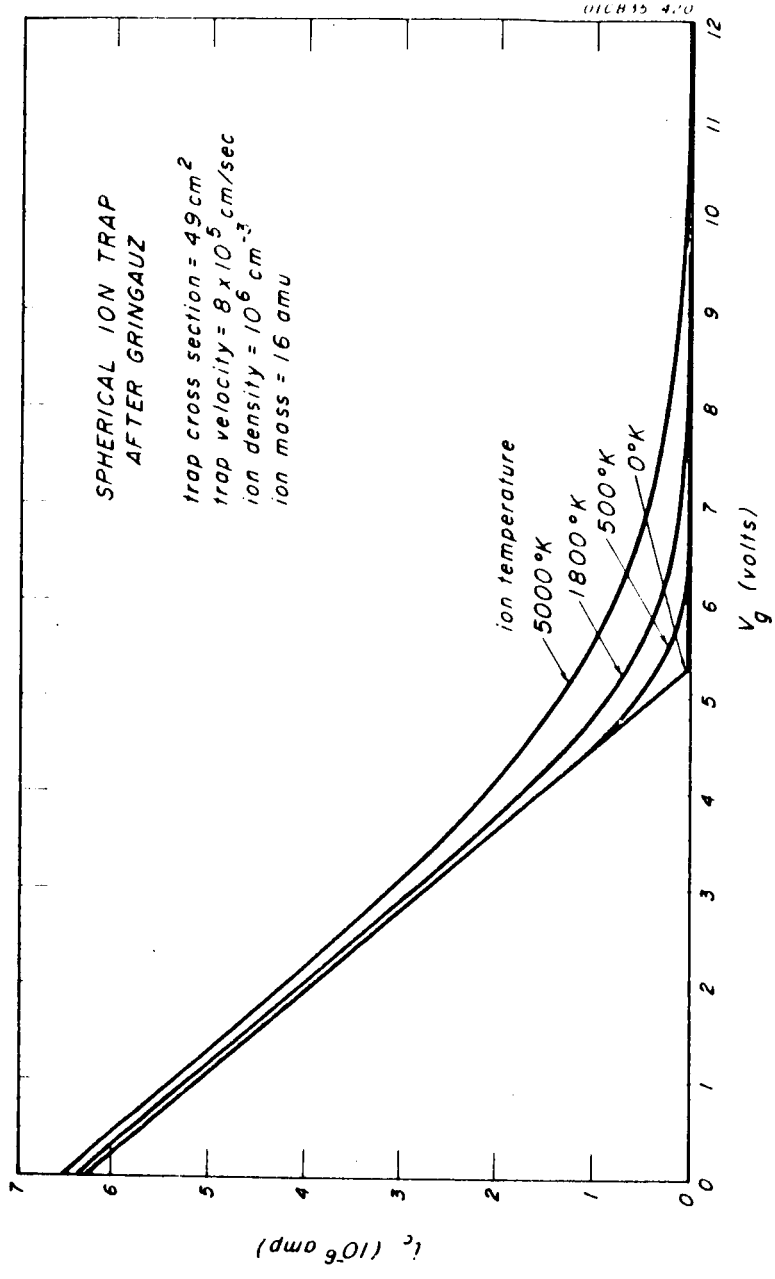

Figure 7. Effect of ion temperature on positive ion current.

collector and grid voltages are programmed to give measurements of both electron and positive ion density and hence subtraction gives the number density of negative ions.

The single-grid ion-traps, like the simple probes, are subject to error due to photoemission from the collector electrode. This may be eliminated by the addition of a second grid (suppressor) between the collector and the outer (control) grid. The suppressor grid is biased negatively with respect to the collector to return photoelectrons to the collector. Multiple-grid ion traps are usually planar, because of the difficulty of fabricating a spherically symmetrical device, and have generally been mounted on the body of the rocket or satellite. Descriptions of planar ion traps have been given by Bourdeau and Donley [14], McKibbin [18], and Hinterreger [19].

The planar ion-traps are exactly equivalent to the spherical configuration and serve also to measure the ion mass-spectrum and the positive ion temperature. The choice between spherical and planar geometry and between boom and body mouting is determined by other factors. The planar device is generally easier to fabricate, particularly if more than one grid is used. The spherical symmetry on the other hand avoids an aspect correction and hence avoids the need for an aspect measurement. The use of a boom allows the ion-trap to be placed outside the space charge sheath of the vehicle and allows the voltage of the outer grid to be swept through plasma potential. Also the use of a boom reduces the time the ion-trap spends in the rarefied wake of the vehicle.

Probe in the D Region

In daytime flights, probe current is first measured at about 50 km and at night at about 75 km. Profiles obtained on four recent flights are shown in Figure 8. Nike Cajun 10.99 was a pre-dawn flight into a quiet ionosphere with sporadic E present (the bifurcated layer between 98 and 102 km). Nike Cajun 10.108 was also a pre-dawn flight but into a disturbed ionosphere (indicated by the ionosonde). Nike Cajun 10.109 was launched at sunset into a quiet ionosphere with sporadic E present (possibly the peak at 110 km). Nike Apache 14.86 gave a typical daytime profile.

The proportionality of probe current to electron density can be justified on theoretical grounds at heights greater than 90 km. The general appearance of these profiles, however, strongly suggests that this proportionality is also true in the lower portions of the profiles. In the daytime profile, the so-called C layer may be identified between 50 and 65 km with the peak at 58 km. The D layer, occurring between 65 and 82 km, corresponds with the absorption of Lyman-α radiation. The nighttime profiles show a generally steeper gradient. Pending further analysis of the operations of the probe and possible comparison with independent techniques, the profile of probe current should be taken to indicate the type of structure that prevails in the D region and the values of electron density should be disregarded.

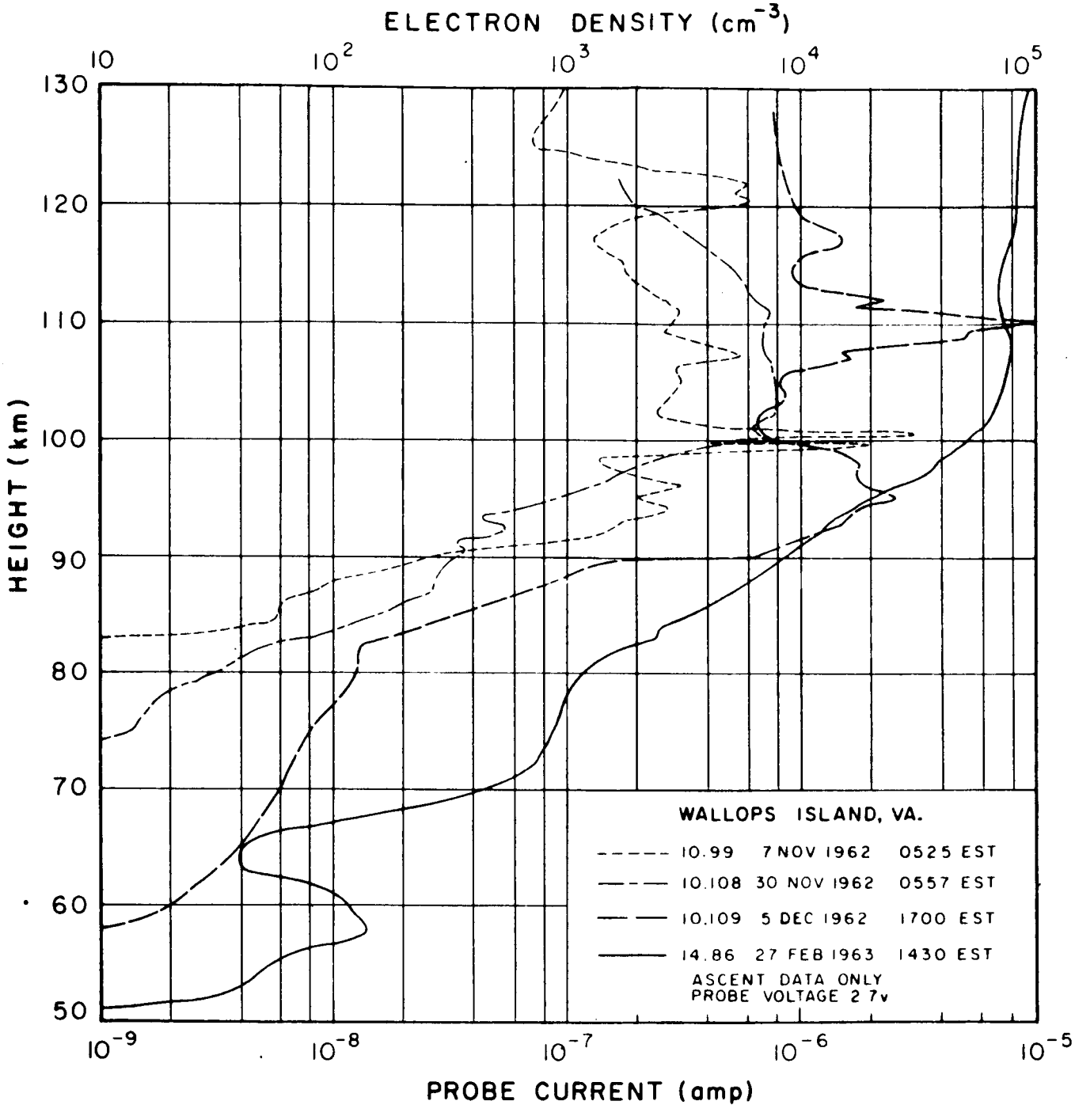

Figure 8. Profiles of probe current in the D and lower E region.

3. INSTRUMENTATION

General Arrangement

The instrument has been constructed in several versions differing in detail but with the same basic circuit arrangement. It has most frequently been used with the nose tip of the rocket as the probing electrode. In some early flights in addition to the nose tip electrode, a circular electrode flush mounted in the cylindrical section of the payload was used. This was found to be unsatisfactory, principally because of its sensitivity to vehicle attitude, and was abandoned in favor of the nose tip position. The appearance of the instrumentation can be seen in Figure 9 which shows two identical payloads — the antennas and housing have been removed from one. These particular payloads are intended to be mounted on the front end of a vapor canister which is, in turn, attached to a Nike Apache rocket.

The circuit of the instrument is shown schematically in Figure 10. The sweep circuit generates the voltage program of Figure 5 which is applied to the electrode. The electrometer converts the probe current to an analog voltage which is the output of the instrument. The voltage of the probe is not telemetered. An ac signal of 540 c/s and amplitude of 100 mv (peak-to-peak) is added to the electrometer output. Each cycle corresponds to a voltage increment of 0.02 volt during the 0.5 second duration of the voltage sweep. The presence of these voltage markers on the telemetry record has been found to facilitate data reduction as well as to increase the accuracy of the measurement.

The instrument is calibrated in flight by substituting a known resistor for the electrode. The calibration relay is energized in either of two ways. In one version, a signal derived from the sweep trigger circuit is used to insert the calibration for 0.5 second at intervals of 32 seconds. In the other, the calibration relay is energized continuously for two periods, each of about 5 seconds, the first starting about 25 seconds after launch and the second starting about 30 seconds before the end of the flight. Two altitude switches, connected as shown in Figure 11, energize the calibration relay between 50,000 and 75,000 feet (15 and 23 km) both on ascent and descent. The same altitude switches have also been used to initiate the timer of a door release mechanism (when used) and to determine trajectory [20]. The altitude switches are vented through four holes, 2 cm in diameter equally spaced on the circumference of the payload. Two of the four vent holes are visible in Figure 9.

The instrument is built in modular form corresponding to the units indicated in the schematic, Figure 10. The battery box and thyrite box are plug-in units for ease in replacement. The sweep generator and trigger circuits and the electrometer and oscillator are constructed on printed cards. The

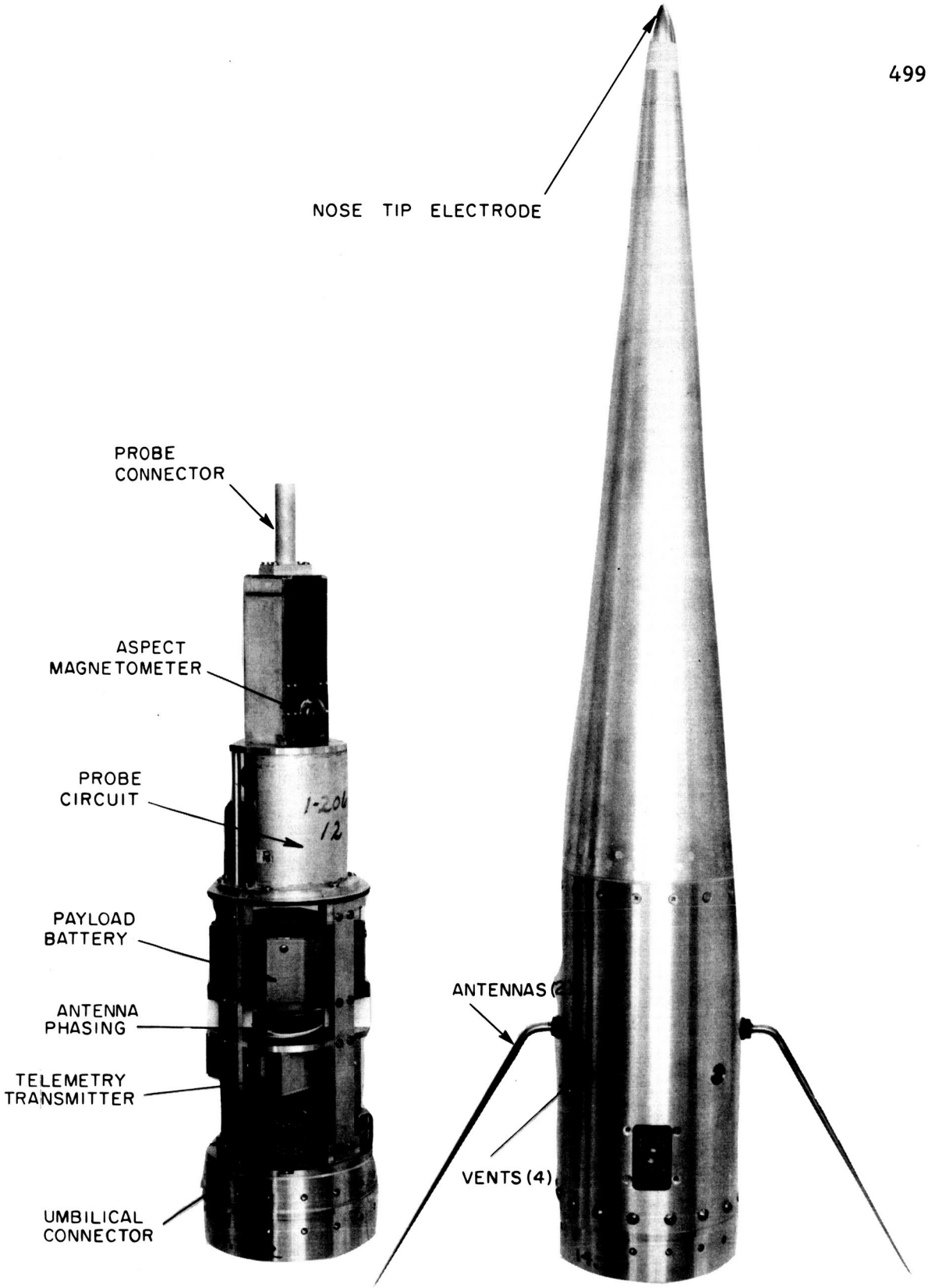

Figure 9. Payloads containing probe instrumentation.

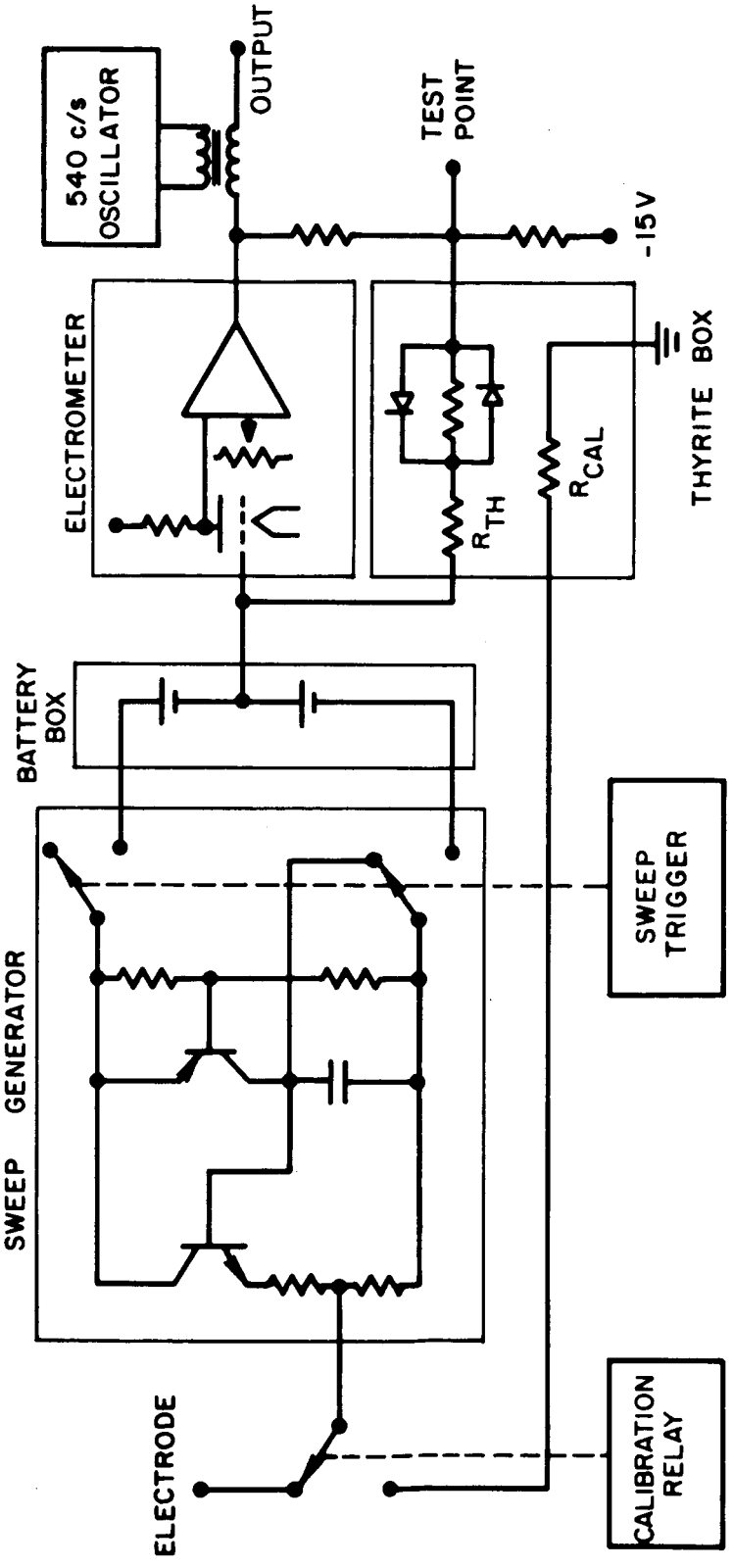

Figure 10. Probe circuit schematic.

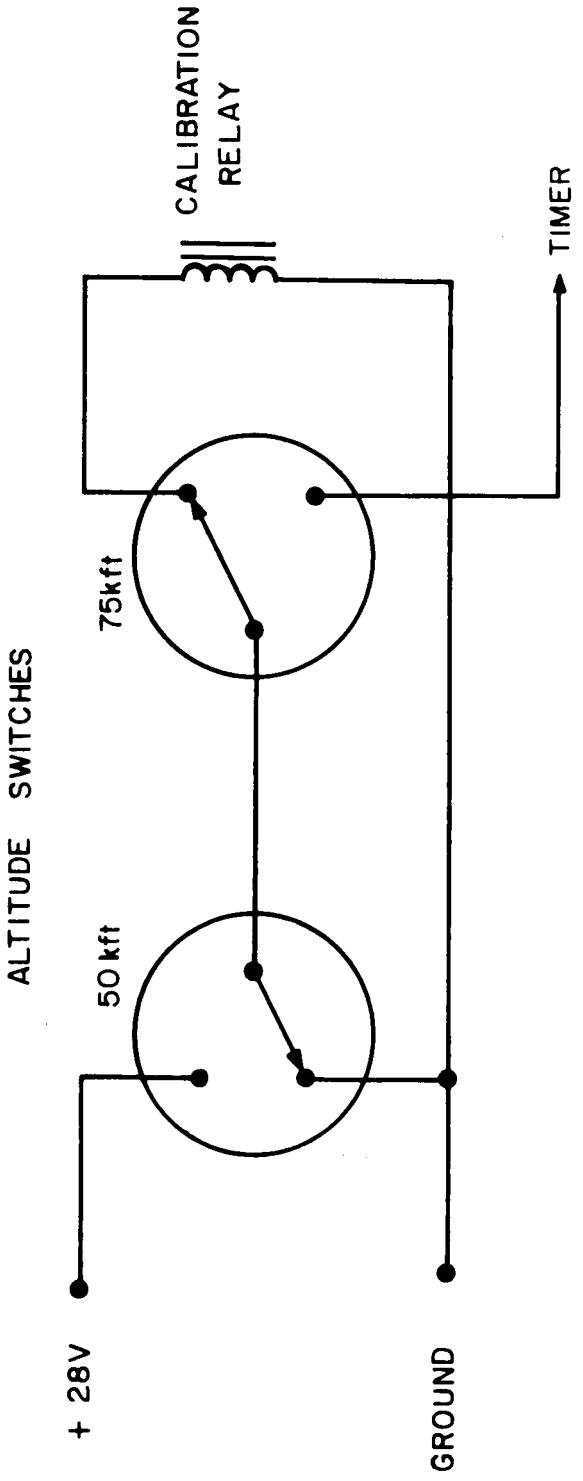

Figure 11. Calibration circuit.

instrument shown in Figure 9 has a base diameter of 13 cm and a height of 14 cm, excluding the probe connector which is itself 8 cm high. The weight of the complete instrument is 1.5 kg.

The instrument is currently being used with an ogive-shaped electrode. Previously a cone-shaped electrode having an included angle of 11 degrees was used but it has been found that the ogive has much less sensitivity to rocket attitude. The construction of the electrode in either case is the same and is illustrated in Figure 12. The electrode assembly replaces the standard nose tip and therefore does not add extra weight to the payload. Electrical connection is made through the rod which mates with a special connector on the instrument and allows a limited amount of relative motion (such as results from thermal expansion of the payload housing).

Sweep Circuit

The complete circuit of the sweep generator and trigger is shown in Figure 13. When the relay closes, the sweep generator is connected to its floating (battery) power supply and the capacitor charges through a constant current circuit (the2N1132 transistor). The electrode is driven by a second transistor (2N929A). When the resistor values indicated by asterisks are adjusted in sequence the correct voltage program can be obtained. The first resistor, nominally 1.5K, is adjusted so that when the capacitor is fully charged the voltage across this resistor is 5.4 volts. Then the second resistor, nominally 33K, is adjusted so that the desired sweep rate of 10.8 volt/sec is obtained at the electrode.

The trigger circuit de-energizes the relay for about 0.1 sec at intervals of 2 seconds. Thus the capacitor is discharged through the 47 ohm resistor and the electrode and sweep circuit are completely disconnected from the electrometer for a momentary zero-check. The trigger circuit uses a unijunction transistor (2N490) for timing and a second transistor (2N1613) for driving the relay. The 2-second interval of the trigger circuit is controlled by the indicated resistor, nominally 180K.

Electrometer Circuit

The circuit of the feedback electrometer is shown in Figure 14. A single-ended arrangement is used. The input tube (Raytheon, CK587) is connected directly to the positive input terminal of a differential amplifier (Philbrick, PP65A). The negative input terminal of the amplifier is used to set the zero of the electrometer. The two diodes in opposition between the input terminals protect the amplifier against large transient signals. The capacitor prevents oscillations within the electrometer. The output of the electrometer is off-set 1 volt by taking the feedback from a voltage divider between the amplifier output and the -15 volt supply.

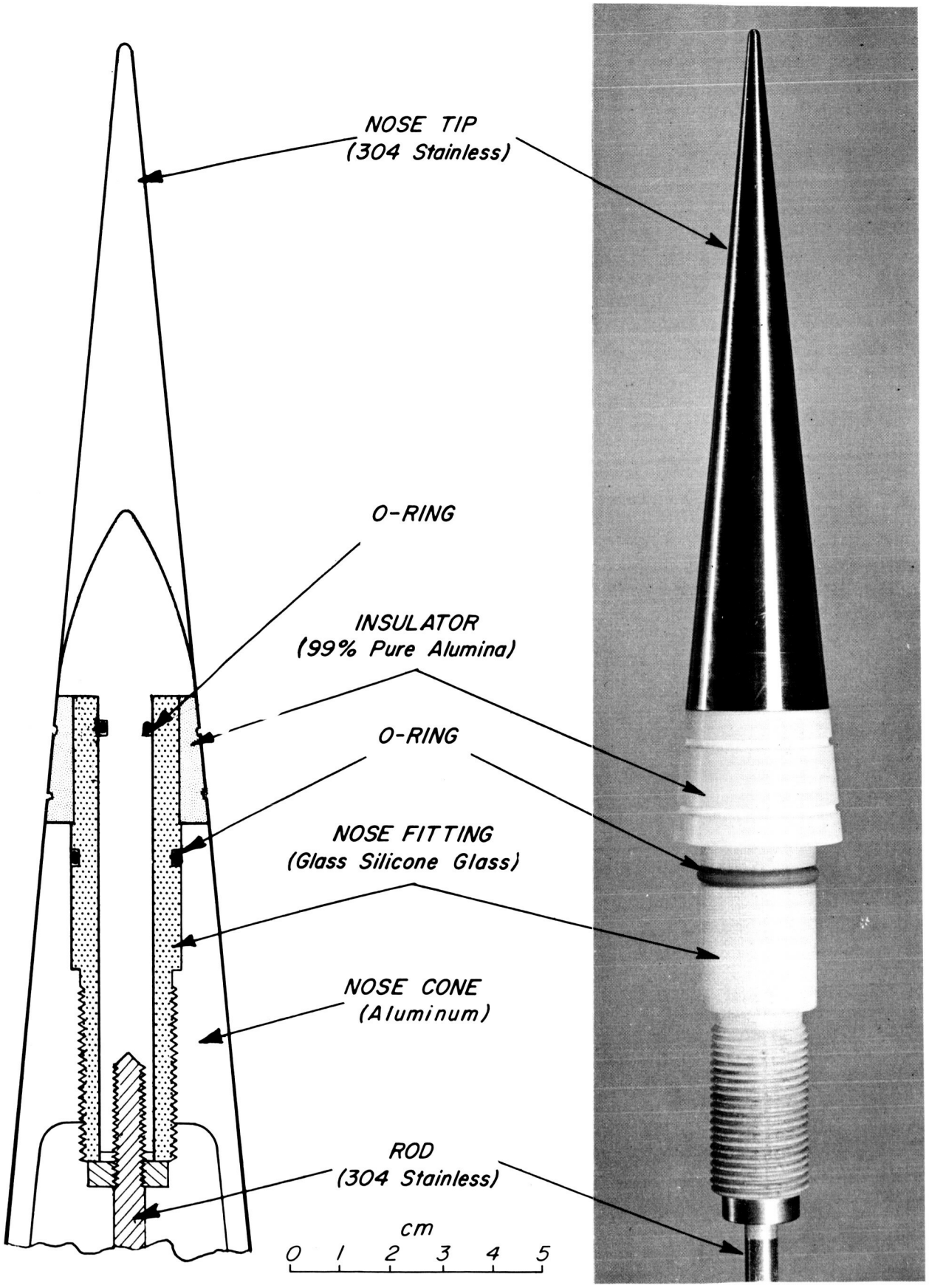

Figure 12. Nose tip electrode.

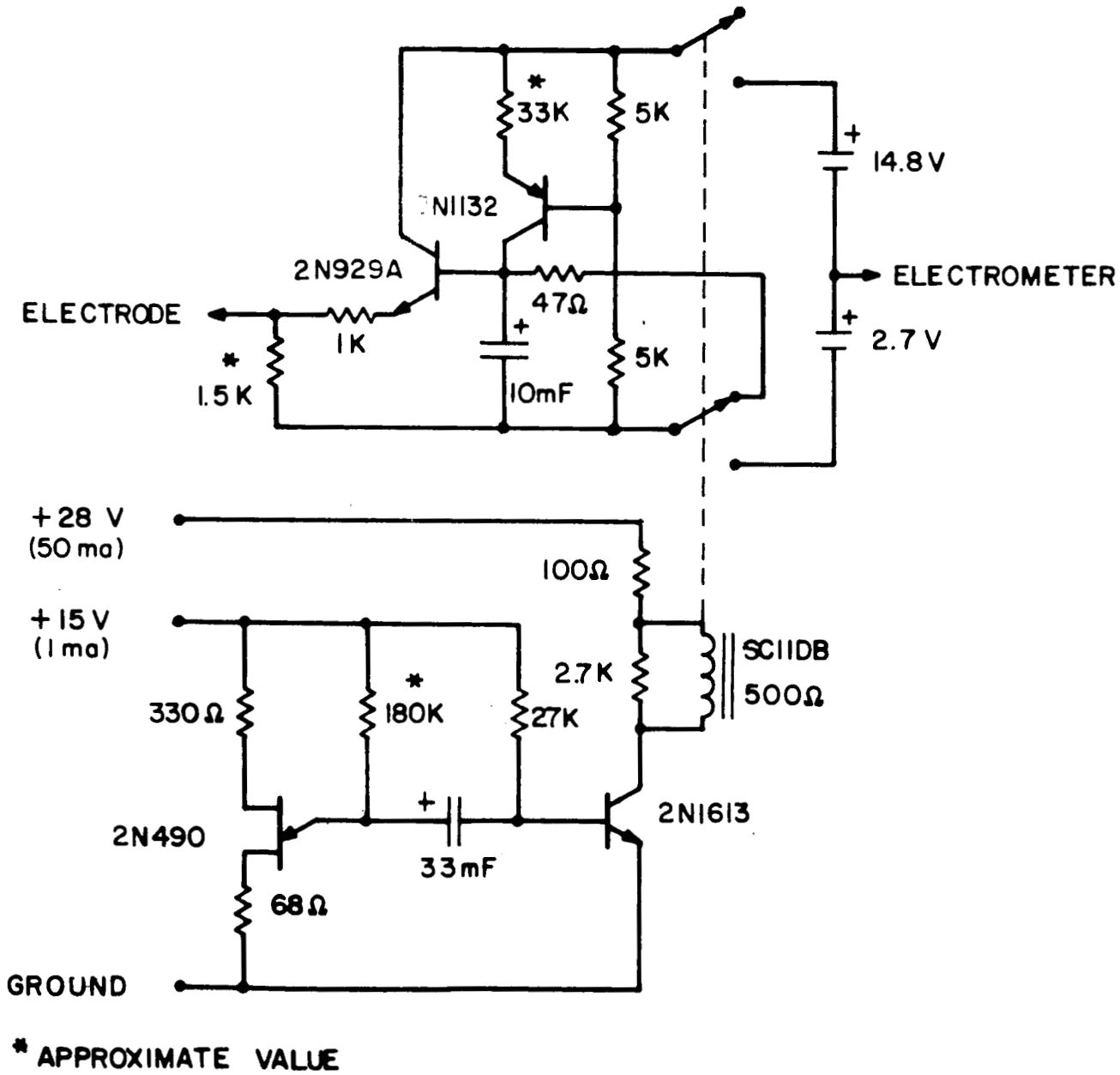

Figure 13. Sweep circuit.

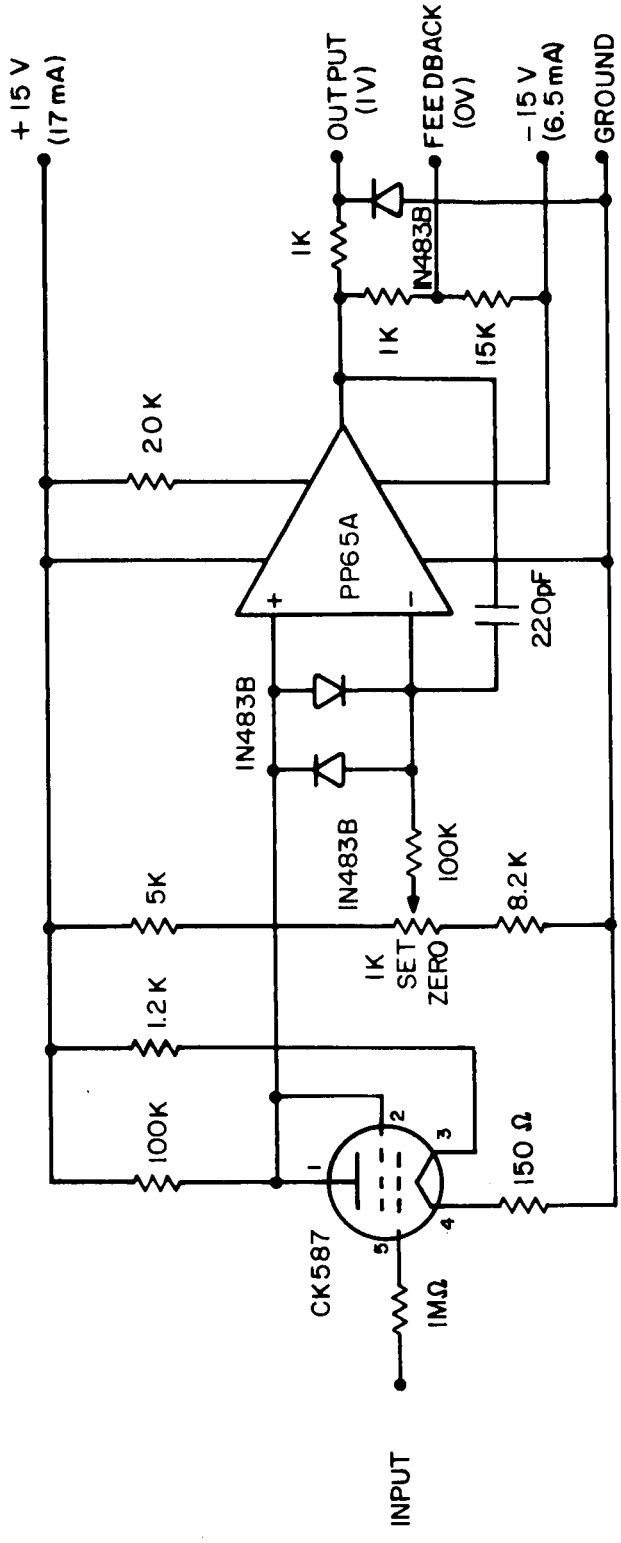

Figure 14. Electrometer circuit.

The feedback element uses a combination of thyrite resistor (General Electric, Magnetic Materials Division) and diodes to produce a compressed scale. The calibration curve of a typical instrument is shown in Figure 15. The off-set of the electrometer output allows the measurement of small positive-ion currents within the limits of 0 to 5 volts prescribed by the standard telemetry system. Some thyrites show a marked polarity effect (i.e., the magnitude of the current depends on the polarity of the applied voltage) and are rejected. Thyrites and diodes are sensitive to temperature; they are therefore thermally shielded and in addition are calibrated during the rocket flight.

Special Notes

The payload housing and rocket motor casing form the second electrode of the bipolar system. Any voltages developed across portions of the external surface must be carefully considered if interference with the operation of the probe is to be avoided. One precaution that has been adopted is to disconnect all signals from the umbilical connector using relays within the payload.

A second possible problem concerns rocket gas which may disturb the ionosphere in the vicinity of the electrode. Trouble from this cause is minimized if the payload is sealed with O-rings at the nose tip (see Figure 12) and if vent holes are provided toward the rear of the payload.

A further precaution which is important is to limit the power of the telemetry transmitter. It has been found on two occasions that rf breakdown at the antennas supresses the probe current. In one case in which a 5 watt transmitter (231.4 mc/s) was used breakdown occurred intermittently between 55 and 80 km. With the power reduced to 2 watts on an otherwise identical flight no breakdown was observed.

Data Reduction

The telemetered signal is always tape recorded at two independent ground stations. At the same time a real-time record is obtained at a chart speed of 10 in/sec and a sensitivity of 1 in/volt. This high-speed record gives the electron temperatures. A slow-speed record is also prepared, generally by play-back of the tape, but sometimes in real-time, at a chart speed of 0.25 in/sec and a sensitivity of 1 in/volt. For this record the normal bandwidth of the telemetry channel is reduced to about 100 c/s. This eliminates the small ac signal which at the slow speed would merely broaden the trace.

The slow-speed record immediately shows the electron density profile. An example, Figure 16, was obtained about one hour before dawn. The record on descent was photographically reversed for easier comparison with the corresponding portion on ascent. The height scale is obtained directly from radar data. The electron density scale is obtained from the pre-flight or

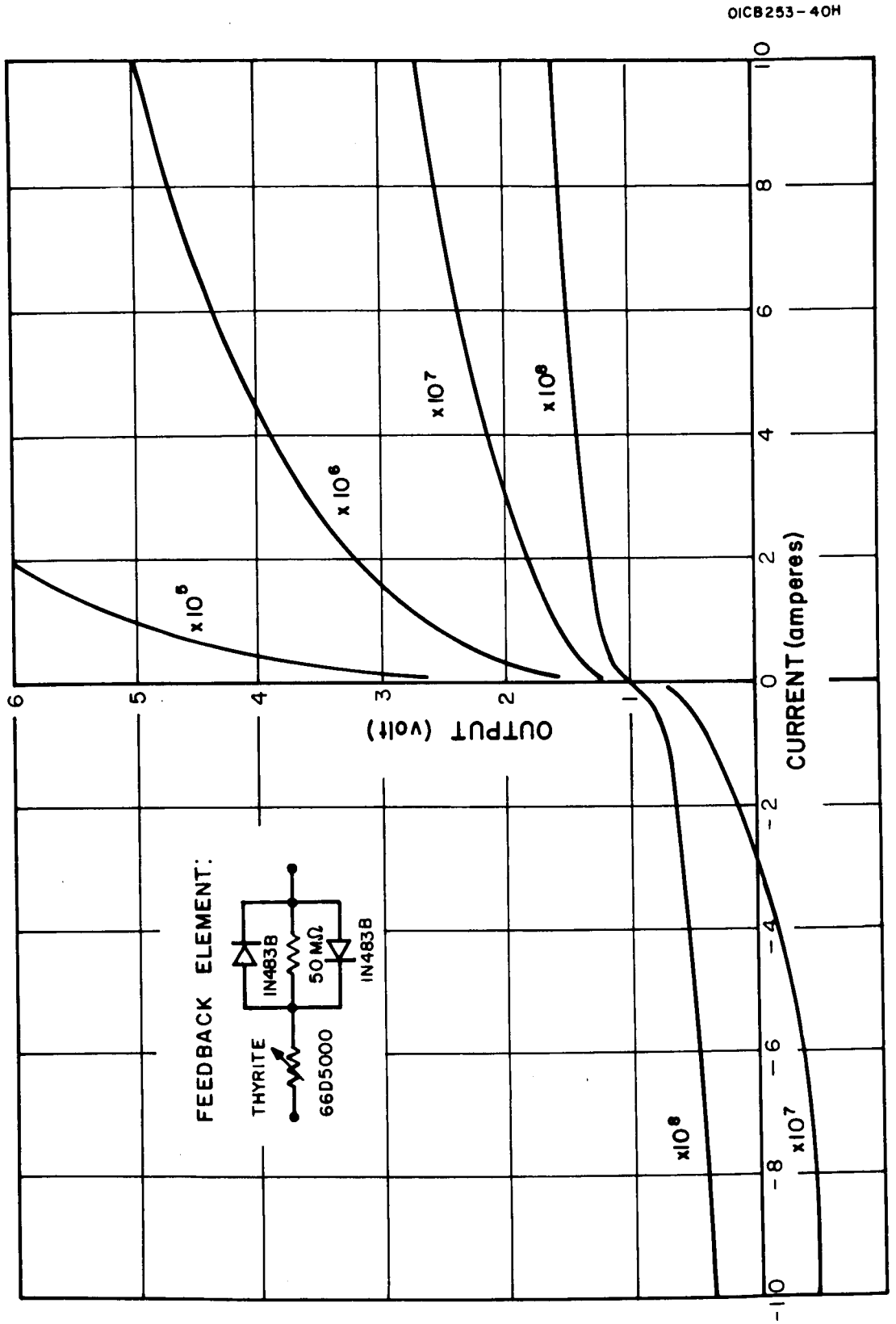

Figure 15. Calibration curve.

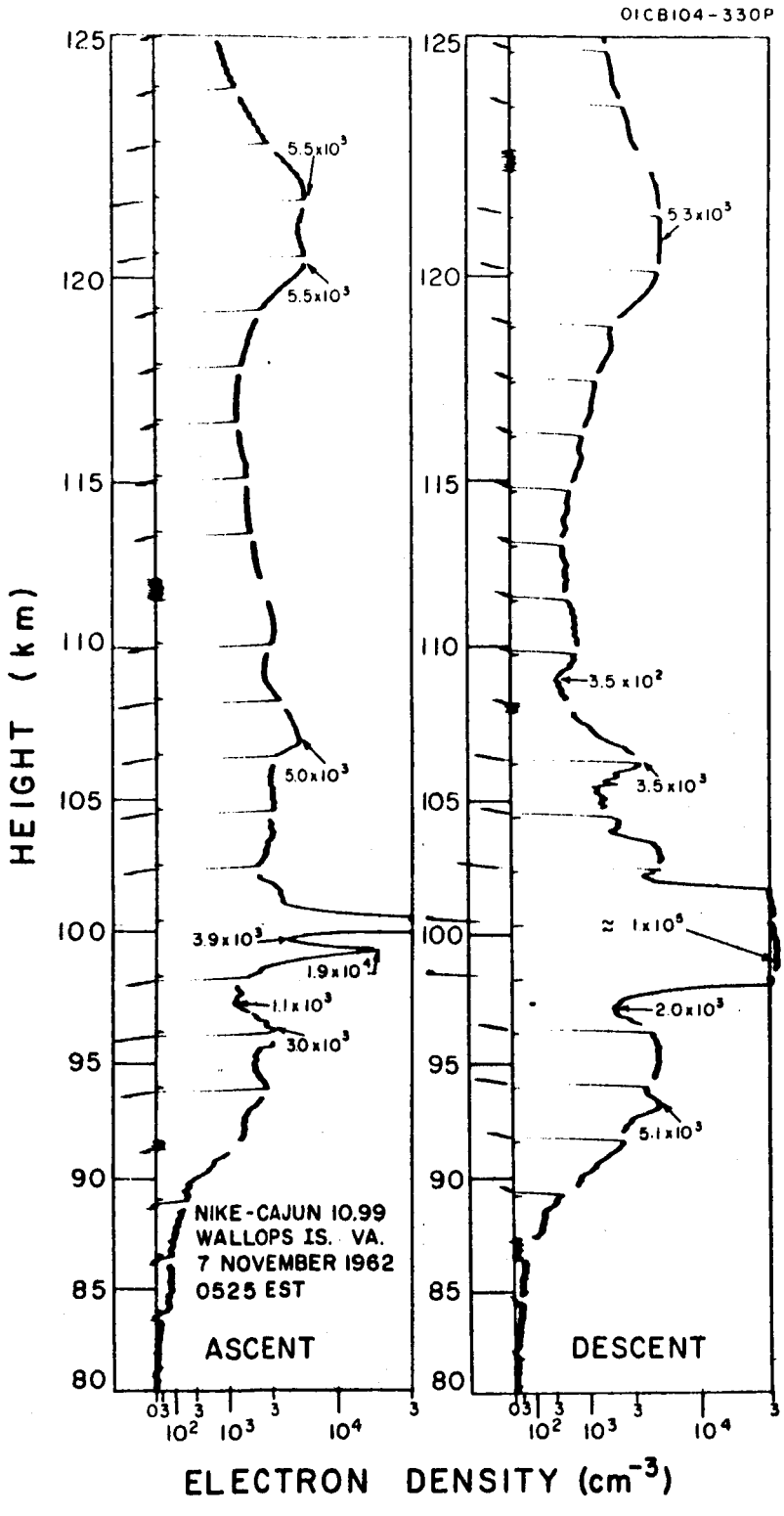

Figure 16. Sections of telemetry record showing electron density profile, 7 November 1962, 0525 EST.

in-flight calibration using a scaling factor obtained from daytime measurements when the absolute value electron density at the peak of the E layer may be obtained from a local ionosonde. The scaling factor used in this case is 1.1×10^{-6} amp equivalent to 1.0×10^{4} cm^{-3}.

The reduction of the data to obtain electron temperature is rather tedious. Individual sweeps of probe voltage must first be measured on the high-speed chart record and a graph prepared of current against voltage. The part of the graph representing collection of positive ions is extrapolated, Figure 17, and subtracted from the total probe current to give electron current. This is then plotted on a conventional semi-log plot as shown in Figure 18. The slope of the linear part of this semi-log plot gives the electron temperature directly. In principle the absolute value of electron density can also be obtained from this plot when the point at which the probe at the potential of the plasma is identified; this is normally taken to be the upper limit of the linear portion of the plot. In practice it is difficult to identify the point accurately because of the gradual curvature of the graph. It is found, in addition, that the absolute values obtained in this way are significantly lower than theory indicates. The discrepancy has not yet been adequately explained and it is recommended that this method of analysis not be used to obtain electron density.

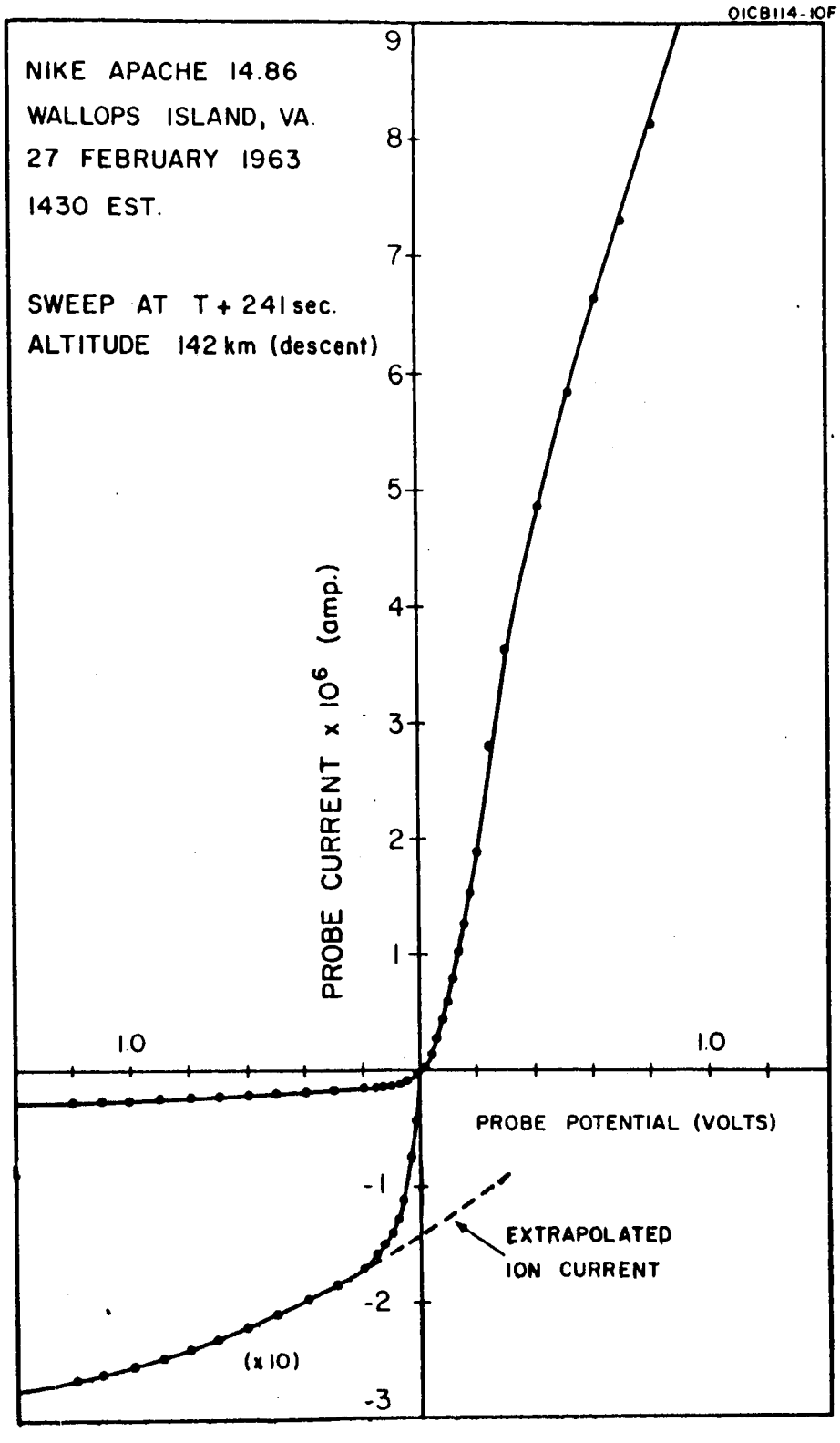

Figure 17. Current-voltage characteristic.

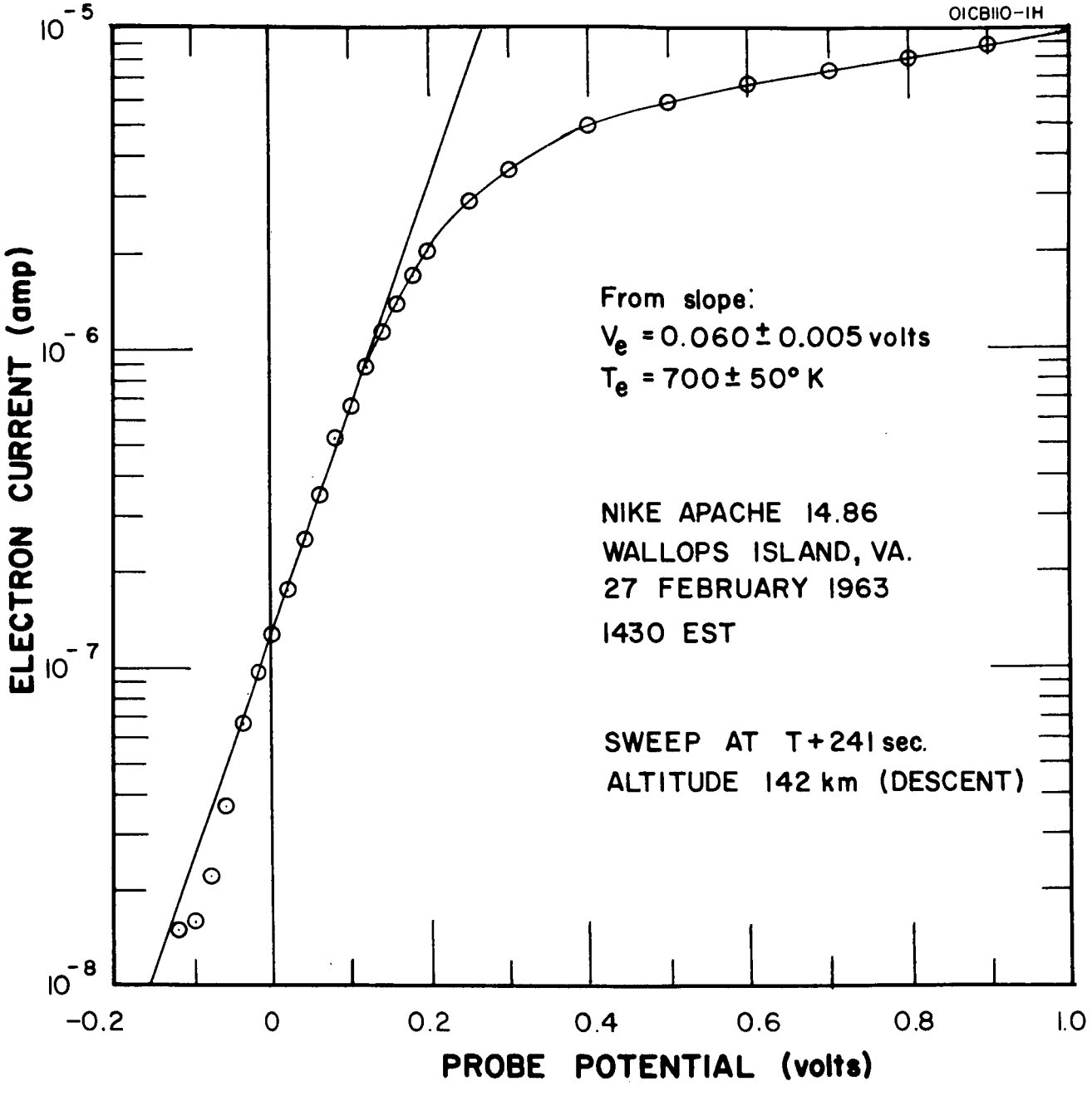

Figure 18. Semi-log plot of electron current vs probe potential.

REFERENCES

1. Hok, G., Spencer, N. W. and Dow, W. G., "Dynamic Probe Measurements in the Ionosphere," J. Geophys. Res. 58, 235-242 (1953).

2. Gringauz, K. I., Bezrukikh, V. V. and Ozerov, V. D., "Results of Measurements of Positive Ion Concentrations in the Ionosphere by Means of Ion Traps on the Third Soviet Earth Satellite," Artificial Earth Satellites, No. 6, Moscow (1961).

3. Langmuir, I. and Mott-Smith, H. M., "Studies of Electric Discharges in Gases at Low Pressures," General Electric Review 27, 449-455, 538-548, 616-623, 762-771, 810-820 (1924).

4. Mott-Smith, H. M. and Langmuir, I., "The Theory of Collectors in Gaseous Discharges," Phys. Rev. 28, 727-763 (1926).

5. Druyvesteyn, M. J., Z. Physik. 64, 781-798 (1930).

6. Branner, G. R., Frair, E. M. and Medicus, G., "Automatic Plotting Device for the Second Derivative of Langmuir Probe Curves," Rev. Sci. Inst. 34, 231-237 (1963).

7. Takayama, K., Ikegami, H. and Miyazaki, S., "Plasma Resonance in a Radio-Frequency Probe," Phys. Rev. Let. 5, 238-240 (1960).

8. Boyd, R. L. F. and Willmore, A. P., "A Method of Studying the Energy Distribution of Ionospheric Ions and Electrons," 1168-1173, Space Research III, (ed. Priester).

9. Johnson, E. O. and Malter, L., "A Floating Double Probe Method for Measurements in Gas Discharges," Phys. Rev. 80, 58-68 (1950).

10. Sagalyn, R. C., Smiddy, M. and Wisnia, J., "Measurement and Interpretation of Ion Density Distributions in the Daytime F Regions," J. Geophys. Rev. 68, 199-211 (1963).

11. Gurevich, A. V., "Perturbations in the Ionosphere Caused by a Moving Body," TRUDY Nr. 17(27), 173-186 (1960).

12. Ichimiya, T., Takayama, K. and Aono, Y., "A Probe for Measuring Ion Density in the Ionosphere," Space Research (ed. Bijl.) North-Holland Publishing Co., Amsterdam, 1960, pp. 397-416.

13. Spencer, N. W., Brace, L. H. and Carignan, G. R., "Electron Temperature Evidence for Nonthermal Equilibrium in the Ionosphere," J. Geophys. Res. 67, 157-175 (1962).

14. Bourdeau, R. E. and Donley, J. L., "Explorer VIII Satellite Measurements in the Upper Atmosphere," Proc. Roy. Soc. 281A, 487-504 (1964).

15. Willmore, A. P., Boyd, R. L. F. and Bowne, P. J., "Some Preliminary Results of the Plasma Probe Experiments on the Satellite Ariel," International Conference on the Ionosphere, July 1962, Institute of Physics and Physical Society, London, 1963.

16. Boyd, R. L. F., "The Collection of Positive Ions by a Probe in an Electrical Discharge," Proc. Roy. Soc. 201, 329-347 (1950).

17. Gringauz, K. I. and Zelikman, M. Kh., "Measurement of the Concentration of Positive Ions Along the Orbit of the Artificial Earth Satellite," Uspekhi Fiz. Nauk. 63, 239-252 (1957).

18. McKibbin, D. D., "A Direct Measurement of Charge Density in the F2 Region," IRE Transactions on Instrumentation, pp. 96-99 (December 1962).

19. Hinteregger, H. E., "Combined Retarding Potential Analysis of Photoelectrons and Environmental Charged Particles up to 234 km," Space Research (ed. Bijl.) North-Holland Publishing Co., Amsterdam, pp. 304-327 (1960).

20. Smith, L. G., "A Simple Method of Trajectory Determination for Sounding Rockets," GCA Technical Report No. 63-9-N (March 1963).

APPENDIX A

THE ASYMMETRICAL BI-POLAR PROBE

Consider an asymmetrical bi-polar probe consisting of two electrodes of unequal surface area between which a potential may be applied and the resulting current measured. It is assumed that (1) the electron velocity distribution is Maxwellian and can be represented by the temperature T and (2) the sheath thickness is small compared with the radius of curvature of the electrodes, so that the current saturates for accelerating potentials.

Initially, with both electrodes at the same potential, the system assumes a negative potential with respect to the plasma, the floating potential, V_f, given by

$$V_f = -(kT_e/e) \log_e (j_e/j_+) \tag{A-1}$$

where k is Boltzmann's constant

T_e the equivalent electron temperature

e the electronic charge

j_e the electron random current density

j_+ the positive ion random current density.

A potential V is applied between the electrodes, V being taken to be positive when the smaller (area A_2) is positive with respect to the larger (area A_1). The potentials of the electrodes assume new values V_1 and V_2, where

$$V = V_2 - V_1 \tag{A-2}$$

The electron currents to the electrodes are, for retarding potentials,

$$i_{e1} = A_1 j_e \exp[eV_1/kT_e] \tag{A-3}$$

$$i_{e2} = A_2 j_e \exp[eV_2/kT_e] \tag{A-4}$$

where the subscripts 1 and 2 refer to the larger and smaller electrode, respectively.

It is convenient at this point to introduce two parameters: the area ratio:

$$\sigma = A_1/A_2 \tag{A-5}$$

and the voltage ratio:

$$\eta = eV/kT_e \tag{A-6}$$

with appropriate subscripts for V being applied to η. Thus η is the potential V expressed as a multiple of the electron energy in voltage units.

Now the positive ion currents to the two electrodes are independent of V_1 and V_2 and have values

$$i_{+1} = A_1 \, j_+ \tag{A-7}$$

and

$$i_{+2} = A_2 \, j_+ \tag{A-8}$$

The total electron current must be numerically equal to the total positive ion current, that is

$$i_{e1} + i_{e2} = i_{+1} + i_{+2} \tag{A-9}$$

From Equations (A-3) and (A-4):

$$i_{e1}/i_{e2} = (A_1/A_2) \exp[e(V_1 - V_2)/kT_e] \tag{A-10}$$

that is

$$i_{e1}/i_{e2} = \sigma \exp[-\eta] \tag{A-11}$$

and from Equations (A-7) and (A-8):

$$i_{+1}/i_{+2} = \sigma \tag{A-12}$$

Finally the probe current i is given by

$$i = i_{+1} - i_{e1} \tag{A-13}$$

Therefore, using Equations (A-9), (A-11), (A-12) and (A-13), we find:

$$i/i_{+1} = \left[\frac{\exp(\eta) - 1}{\exp(\eta) + \sigma}\right] \tag{A-14}$$

This is the mathematical formulation of the current-voltage characteristic of an asymmetrical bi-polar probe having an area ratio $\sigma(\geq 1)$. It is plotted in Figure A-1 for values of σ of 1, 10, 100, and 1000. The curve for the symmetrical bi-polar probe ($\sigma = 1$) is point symmetric about the origin (only the

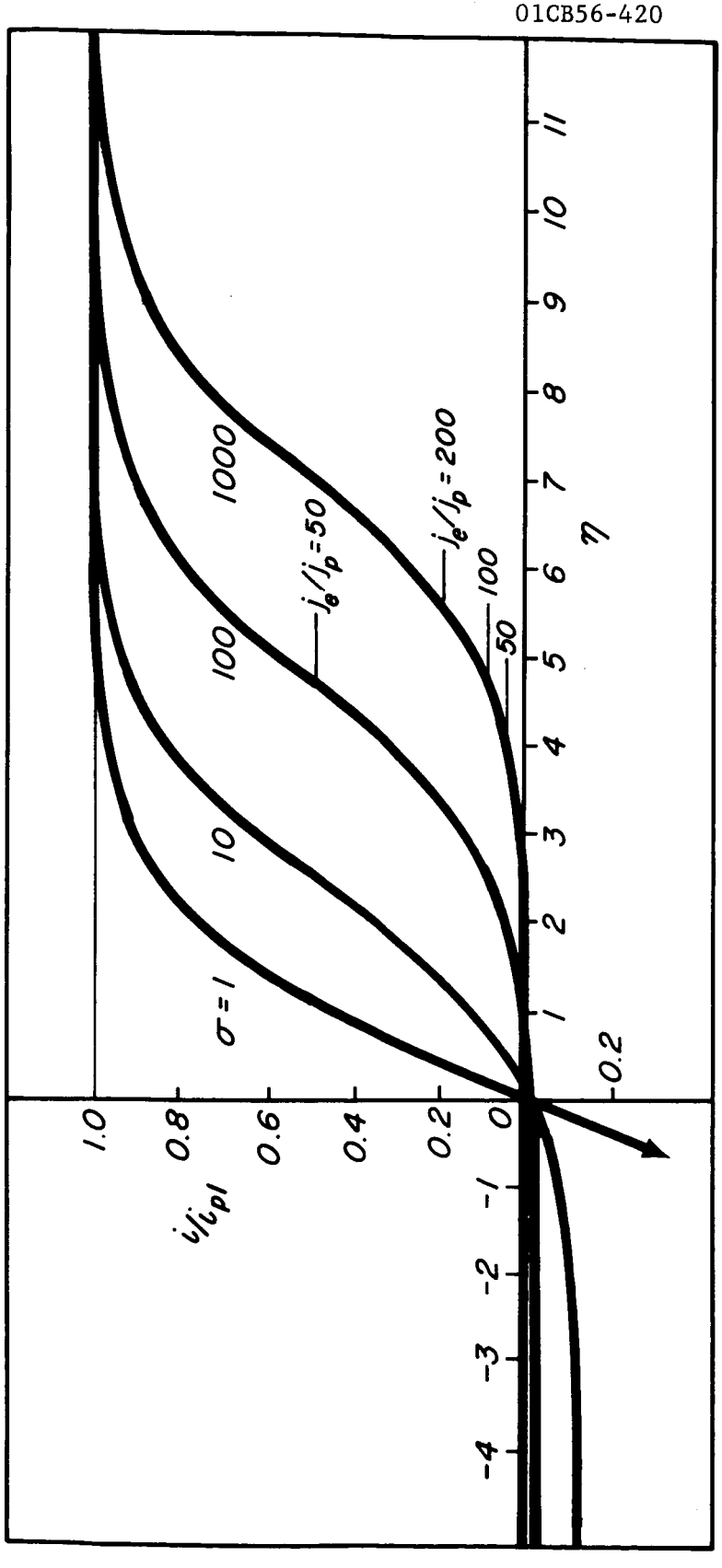

Figure A-1. Current-voltage characteristics for four values of area ratio.

positive half is shown). For values of σ greater than 100, the curves become point symmetric about the point

$$i/i_{+1} = 0.5 \tag{A-15}$$

and

$$\eta = \log_e (2 + \sigma). \tag{A-16}$$

We must now introduce the restriction that the above analysis is valid only for retarding potentials on the electrodes. For accelerating potentials, the electron current is limited to the random current density. Now the potentials of the two electrodes, η_1 and η_2, are given by

$$\exp(-\eta_1) = (j_e/j_+) \frac{\sigma + \exp(\eta)}{\sigma + 1} \tag{A-17}$$

and

$$\exp(-\eta_2) = (j_e/j_+) \frac{\sigma \exp(-\eta) + 1}{\sigma + 1} \tag{A-18}$$

Saturation occurs when the smaller electrode reaches space potential ($\eta_2 = 0$) at a value of η given by

$$\exp(\eta) = \frac{\sigma(j_e/j_+)}{\sigma + 1 - (j_e/j_+)} \tag{A-19}$$

and a value of i given by

$$i/i_{+1} = (j_e/j_+ - 1)/\sigma \tag{A-20}$$

If $\sigma < (j_e/j_+ - 1)$, no electron current saturation occurs.

The point at which electron current saturation occurs is thus determined by the area ratio σ and the random current density ratio j_e/j_+. The short horizontal lines in Figure A-1 indicate electron current saturation. In the ionosphere the value of j_e/j_+ is computed to be about 200.

The floating potential $\eta_f (= eV_f/kT_e)$ is from Equation (A-1),

$$\exp(\eta_f) = j_e/j_+ \tag{A-21}$$

and therefore, as might be expected, for very large σ ($\gg j_e/j_+$) the smaller electrode saturates when η is equal to the floating potential. In other words, for sufficiently large σ the smaller electrode is essentially a single probe and the larger electrode maintains a constant potential equal to the floating

potential. We may determine how large σ must be for such a simplification to be made; it evidently must be several times the value of j_e/j_+. In Figure A-2 the curves of Figure A-1 are replotted on semi-log paper in the manner used on deriving electron temperature. On this plot the ordinate is

$$\Delta i/i_{+1} = (i + i_{+2})/i_{+1} \tag{A-22}$$

The single Langmuir probe is characterized by a linear plot on semi-log paper. It is seen in Figure A-1 that for all values of σ the plots are very close to linear for $\Delta i/i_{+1} \leq 0.1$. Now electron saturation occurs at $\Delta i/i_{+1} = (j_e/j_+)/\sigma$. Therefore the condition that the asymmetrical bi-polar probe may be analyzed as a single probe is

$$\sigma \geq 10\ (j_e/j_+). \tag{A-23}$$

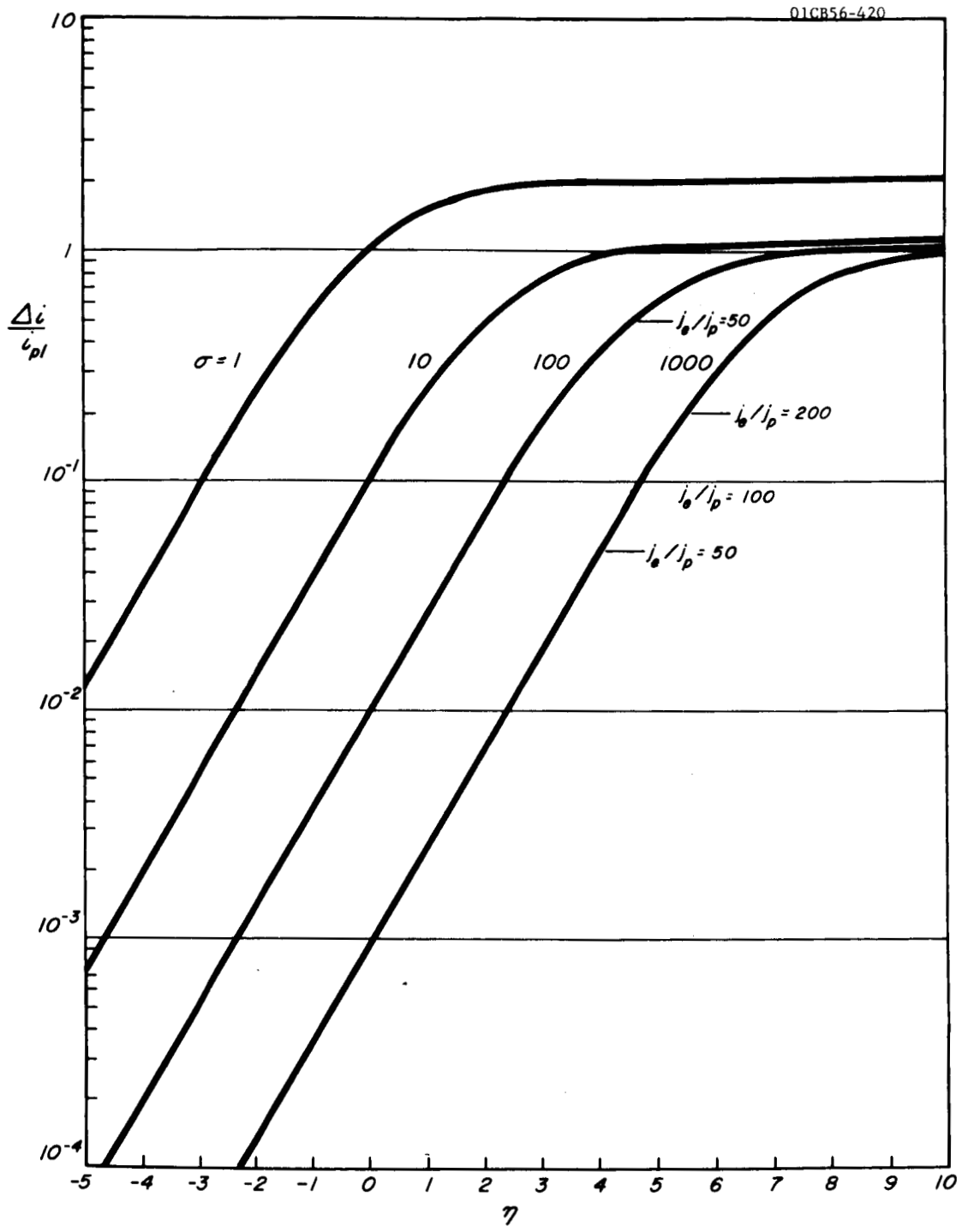

Figure A-2. Semi-log plot of current-voltage characteristics for bi-polar probes.